Human (α2→6) and avian (α2→3) sialylated receptors of influenza A virus show distinct conformations and dynamic in solution

Guilherme L. Sassaki [†,1,‡], Stefano Elli [†,1], Timothy R. Rudd [†,1,§], Eleonora Macchi [1], Edwin A. Yates [2], Annamaria Naggi [1], Zachary Shriver [3], Rahul Raman [3], Ram Sasisekharan [3], Giangiacomo Torri [1] and Marco Guerrini [1,*].

[1] Istituto di Ricerche Chimiche e Biochimiche "G. Ronzoni", Via Giuseppe Colombo,81 Milano 20133 ITALIA
[2] Institute of Integrative Biology, Biosciences Building, University of Liverpool, Crown Street, Liverpool L69 7ZB UK
[3] Harvard-MIT Division of Health Sciences and Technology, Koch Institute for Integrative Cancer Research, Department of Biological Engineering, Massachusetts Institute of Technology, Cambridge, MA 02139 USA

Current Location:
[‡] Departamento de Bioquimica e Biologia Molecular, Universidade Federal do Paraná, CP 19.046, CEP81.531-980 Curitiba, PR, Brasil
[§] Diamond Light Source Ltd, Diamond House, Harwell Science & Innovation Campus, Didcot, Oxfordshire OX11 0DE UK

[*]To whom correspondence should be addressed; E-mail: guerrini@ronzoni.it, Tel: +39-2-70641627

[†]These authors contributed equally to the paper

Suppl. Table 1. *^{1}H and ^{13}C NMR assignments of LSTa and LSTc (δ values in ppm at 295 K).*
Suppl. Table 2. *Spin-lattice and spin-spin relaxation times (T1 and T2 values in ms) and heteronuclear NOEs of LSTa and LSTc.*
Suppl. Table 3. *Selected experimental and predicted inter-proton distances from LSTa and LSTc.*
Suppl. Table 4. *Comparison between measured and simulated (NOEPROM) inter-residue proton-proton percentage NOE signals (%NOE).*
Suppl. Table 5. *Torsional states of LSTa and LSTc conformers selected by $RMSD_{exp}$ analysis.*
Suppl. Table 6. *LSTc and LSTa hydrogen bond networks.*
Suppl. Table 7. *Experimental and calculated $^{3}J_{CH}$ interglycosidic coupling constant (Hz) for LSTa and LSTc.*

Suppl. Fig. 1. *Scheme of human milk lactosyl sialyl-N-tetraoses.*
Suppl. Fig. 2. *2D Partial TOCSY spectra of NH coupling spin systems from Neu5Ac and GlcNAc at 278 K.*
Suppl. Fig. 3.*Example of signal assignment of a sensitivity-enhanced HSQC spectrum using cross peaks generated by homonuclear proton coupling.*
Suppl. Fig. 4. *Experimental curves of NH $\Delta\upsilon_{½}$ [Hz] plotted against temperature [K].*
Suppl. Fig. 5. *2D Partial NOESY (300 ms at 295 K) spectrum of LSTc.*
Suppl. Fig. 6. *J-HMBC and HSQC spectra of LSTa and LSTc.*
Suppl. Fig. 7. *End-to-End length analysis of LSTc over the MD simulation, 100 ns, 295 K.*
Suppl. Fig. 8. *End-to-End length analysis of LSTa over the MD simulation, 100 ns, 295 K.*
Suppl. Fig. 9. *LSTc θ angle. A. θ angle, B. density of θ angle.*
Suppl. Fig. 10. *LSTa θ angle. A. θ angle, B. density of θ angle.*
Suppl. Fig. 11. *LSTc ω angle. A. ω angle, B. density of ω angle.*
Suppl. Fig. 12. *Glycosidic torsionals angles of LSTc at 295, 395 and 495 K.*
Suppl. Fig. 13. *Glycosidic torsionals angles of LSTa at 295, 395 and 495 K.*
Suppl. Fig. 14. *RMSD analysis of LSTc over the MD simulation, 100 ns, 295 K.*
Suppl. Fig. 15. *RMSD analysis of LSTa over the MD simulation, 100 ns, 295 K.*
Suppl. Fig. 16. *Glycosidic torsionals angles of LSTc with conformers from the different RMSD populations highlighted.*
Suppl. Fig. 17. *Glycosidic torsionals angles of LSTa with conformers from the different RMSD populations highlighted.*
Suppl. Fig. 18. *LSTc $RMSD_{exp}$ analysis. A. $RMSD_{exp}$, B. $RMSD_{exp}$ density.*
Suppl. Fig. 19. *LSTc Glycosidic torsionals angles with conformers from the different $RMSD_{exp}$ populations highlighted.*
Suppl. Fig. 20. *LSTa $RMSD_{exp}$ analysis. A. $RMSD_{exp}$, B. $RMSD_{exp}$ density.*
Suppl. Fig. 21. *LSTa Glycosidic torsionals angles with conformers from the different $RMSD_{exp}$ populations highlighted.*
Suppl. Fig. 22. *Glycosidic torsionals angles of LSTc with conformers from the different θ angle populations highlighted.*
Suppl. Fig. 23. *Glycosidic torsionals angles of LSTa with conformers from the different θ angle populations highlighted.*
Suppl. Fig. 24. *RMSIP of the eigenvectors (first ten) derived by PCA of the LSTc (**A.**) and LSTa (**B.**) MD simulations.*
Suppl. Fig. 25. *PCA Scree plot for the analyses of the LSTc (**A.**) and LSTa (**B.**) MD simulations.*
Suppl. Fig. 26. *PCA Loading plot for the analysis of the LSTc MD simulation.*
Suppl. Fig. 27. *PCA Loading plot for the analysis of the LSTa MD simulation.*
Suppl. Fig. 28. *PCA normalised eigenvector plot for the analysis of the LSTc MD simulation.*
Suppl. Fig. 29. *PCA normalised eigenvector plot for the analysis of the LSTa MD simulation.*
Suppl. Fig. 30. *Porcupine plot representations of the first four eigenvectors for LSTc.*
Suppl. Fig. 31. *Porcupine plot representations of the first four eigenvectors for LSTa.*
Suppl. Fig. 32. *LSTc MD PCA Loading plot, with conformers from the different RMSD populations highlighted.*
Suppl. Fig. 33. *LSTa MD PCA Loading plot, with conformers from the different RMSD populations highlighted.*
Suppl. Fig. 34. *LSTc MD PCA Loading plot, with conformers from the different θ angle populations highlighted.*
Suppl. Fig. 35. *LSTa MD PCA Loading plot, with conformers from the different θ angle populations highlighted.*
Suppl. Fig. 36. *LSTc MD PCA Loading plot,with conformers from the different $RMSD_{exp}$ populations highlighted.*
Suppl. Fig. 37. *LSTc MD PCA Loading plot,with conformers from the different $RMSD_{exp}$ populations highlighted.*
Suppl. Fig. 38. *Proposed hydrogen bond network for LSTc and LSTa $RMSD_{exp}$ max conformers.*

Supplementary Table 1. ^{1}H and ^{13}C NMR assignments of LSTa and LSTc (δ values in ppm at 295 K).

			LSTa			
$^{1}H/^{13}C$	**NeuAc5**	**Gal-1**	**GlcNAc**	**Gal-2**	**Glcα**	**Glcβ**
1	176.7	4.513/105.9	4.739/105.1	4.446/105.6	5.227/94.4	4.665/98.3
2	102.3	3.530/71.7	3.898/57.2	3.584/72.6	3.580/73.7	3.256/76.3
3	1.782_{ax};2.751_{eq}/42.3	4.082/78.2	3.817/84.7	3.745/84.5	3.821/74.0	3.638/76.9
4	3.683/70.9	3.932/69.8	3.565/71.08	4.145/70.9	3.644/81.0	3.644/81.0
5	3.834/54.2	3.677/77.7	3.485/77.8	3.717/77.5	3.944/72.7	3.603/77.4
6	3.627/75.4	3.727^{a};3.771^{b}/63.6	3.892^{a};3.782^{b}/63.1	3.727^{a};3.771^{b}/63.6	3.853^{a};3.85^{b}/62.5	3.948^{a};3.841^{b}/62.6
7	3.596/70.6		2.028/24.9			
8	3.862/74.4		177.6			
9	3.836^{a};3.639^{b}/65.0					
10	2.028/24.8					
11	177.6, $_{1770(11)/22.2(9)\ T1/T2}$					
NH	8.181, $^{1}J_{H-H}$9.90					
NH			8.480, $^{1}J_{H-H}$ 10.08			
			LSTc			
$^{1}H/^{13}C$	**NeuAc5**	**Gal-1**	**GlcNAc**	**Gal-2**	**Glcα**	**Glcβ**
1	176.2	4.451/105.9	4.73/105.2	4.445/105.5	5.220/94.4	4.664/98.3
2	102.7	3.534/73.3	3.802/57.3	3.583/72.6	3.580/73.7	3.287/76.4
3	1.711_{ax}; 2.665_{eq}/42.3	3.671/74.9	3.777/74.9	3.738/84.6	3.820/74.0	3.639/76.94
4	3.654/70.7	3.926/70.1	3.663/82.9	4.158/70.9	3.649/80.9	3.649/80.9
5	3.800/54.5	3.818/76.3	3.601/77.3	3.720/77.4	3.947/72.7	3.608/76.94
6	3.702/75.1	3.983^{a};3.544^{b}/66.0	3.950^{a};3.842^{b}/62.65	3.7726a;3.7461b/63.55	3.879^{a};3.842^{b}/62.51	3.952^{a};3.792^{b}/62.58
7	3.553/71.1		2.050/24.9			
8	3.887/74.3		177.6			
9	3.870^{a};3.636^{b}/65.2					
10	2.025/24.7					
11	177.6, $_{2172(9)/41(8)\ T1/T2}$					
NH	8.165, $^{1}J_{H-H}$ 9.55					
NH			8.403, $^{1}J_{H-H}$ 9.49			

$^{a, b}$ Chemical shifts of protons linked directly to the carbon nucleus. (HSQC,HSQC-TOCSY,TOCSY. HMBC and NOESY experiments).

Supplementary Table 2. Spin-lattice and spin-spin relaxation times (T1 and T2 values in ms) and hetero-nuclear NOEs of LSTa and LSTc measured at 600 MHz in aqueous solution at 295 K.

LSTa	T1	T2	$R_{T1/T2}$	**NOE**	**LSTc**	T1	T2	$R_{T1/T2}$	NOE
C3-axNeu	159(4)	135(2)	1.18(3)	1.50	C3-axNeu	157(3)	138(2)	1.14(2)	1.75
C3-eqNeu	162(5)	151(5)	1.07(5)	1.91	C3-eqNeu	140(3)	155(3)	0.90(3)	1.79
C4-Neu	339(6)	302(9)	1.12(5)	1.69	C4-Neu	331(4)	299(5)	1.11(3)	1.79
C5-Neu	327(3)	365(14)	0.90(4)	1.69	C5-Neu	341(5)	218(12)	1.56(10)	1.76
C6-Neu	328(3)	302(1)	1.09(1)	1.65	C6-Neu	335(6)	235(3)	1.43(4)	1.77
C7-Neu	284(4)	238(4)	1.19(3)	1.60	C7-Neu	315(5)	270(2)	1.17(2)	1.59
C8-Neu	345(7)	306(3)	1.13(3)	1.62	C8-Neu	361(5)	329(15)	1.10(6)	1.86
C9-Neuα	234.(11)	200(7)	1.17(9)	1.79	C9-Neuα	230(4)	209(5)	1.10(5)	1.93
C9-Neuβ	230(13)	190(6)	1.21(10)	1.81	C9-Neuβ	230(4)	209(5)	1.10(5)	1.93
CH_3-NAcNeu	1770(11)	22.2(9)	79.7(10)	1.26	CH_3-NAcNeu	2172(9)	41(8)	52.9(8)	1.13
C1-Gal1	329(4)	213(5)	1.54(5)	1.60	C1-Gal1	352(7)	258(6)	1.36(5)	1.62
C2-Gal1	337(8)	211(7)	1.60(9)	1.64	C2-Gal1	330(3)	277(7)	1.19(4)	1.57
C3-Gal1	289(6)	205(3)	1.41(5)	1.67	C3-Gal1	340(5)	233(6)	1.46(5)	1.44
C4-Gal1	299(2)	257(7)	1.16(4)	1.57	C4-Gal1	297(7)	261(2)	1.14(3)	1.45
C5-Gal1	351(4)	258(6)	1.36(5)	1.69	C5-Gal1	320(5)	247(9)	1.30(6)	1.64
C6-Gal1α	220(5)	203(7)	1.08(6)	1.76	C6-Gal1α	176(7)	135(3)	1.30(8)	1.51
C6-Gal1β	220(6)	203(8)	1.08(7)	1.76	C6-Gal1β	192(15)	150(3)	1.28(12)	1.41
C1-GlcNAc	323(7)	238(5)	1.36(5)	1.60	C1-GlcNAc	335(4)	267(4)	1.25(3)	1.65
C2-GlcNAc	296(6)	240(7)	1.23(6)	1.69	C2-GlcNAc	326(7)	226(8)	1.44(8)	1.67
C3-GlcNAc	318(10)	193(6)	1.65(10)	1.53	C3-GlcNAc	329(5)	266(8)	1.24(5)	1.71
C4-GlcNAc	316(7)	328(8)	0.96(8)	1.62	C4-GlcNAc	324(8)	176(2)	1.84(6)	1.62
C5-GlcNAc	324(5)	234(7)	1.38(6)	1.62	C5-GlcNAc	418(7)	224(10)	1.87(11)	1.68
C6-GlcNAcα	220(6)	203(8)	1.08(7)	1.76	C6-GlcNAcα	263(9)	224(5)	1.17(6)	1.86
C6-GlcNAcb	220(7)	203(6)	1.08(6)	1.76	C6-GlcNAcβ	263(5)	216(5)	1.22(5)	1.44
CH_3-GlcNAc	1770(11)	22.2(9)	79.7(10)	1.26	CH_3-GlcNAc	2190(8)	23.2(10)	94.4(9)	1.93
C1-Gal2	333(7)	269(8)	1.24(6)	1.76	C1-Gal2	374(4)	153(3)	2.44(7)	1.80
C2-Gal2	362(9)	314(9)	1.15(6)	1.83	C2-Gal2	359(1)	310(5)	1.16(2)	1.74
C3-Gal2	334(6)	214(8)	1.56(8)	1.67	C3-Gal2	335(4)	249(4)	1.35(3)	1.78
C4-Gal2	354(5)	379(6)	0.93(2)	1.64	C4-Gal2	318(3)	342(3)	0.93(1)	1.62
C5-Gal2	348(6)	264(4)	1.32(4)	1.88	C5-Gal2	365(5)	297(7)	1.23(4)	1.81
C1-Glcα	319(6)	329(6)	0.97(3)	1.60	C1-Glcα	340(5)	306(9)	1.11(4)	1.54
C2-Glcα	442(6)	334(6)	1.32(4)	1.98	C2-Glcα	455(6)	502(5)	0.91(5)	1.83
C3-Glcα	433(10)	389(23)	1.11(9)	1.97	C3-Glcα	395(7)	385(6)	1.03(3)	2.00
C4-Glcαβ	385(5)	275(5)	1.40(4)	1.86	C4-Glcαβ	416(7)	249(3)	1.67(4)	1.86
C5-Glcα	429(6)	351(7)	1.22(6)	1.82	C5-Glcα	414(4)	485(10)	0.85(2)	1.90
C1-Glcβ	434(6)	403(7)	1.08(6)	1.86	C1-Glcβ	470(5)	372(11)	1.26(5)	1.86
C2-Glcβ	444(11)	402(7)	1.10(9)	1.76	C2-Glcβ	458(8)	411(5)	1.11(3)	1.93
C6-Glcβα	285(13)	194(1)	1.47(7)	1.67	C6-Glcβα	191(6)	191(3)	1.00(4)	1.79

Supplementary Table 3. Selected experimental and predicted intra-residue proton-proton distances from LSTa and LSTc.

LSTa	**Neu5Ac(*)**	**Gal1**	**GlcNAc**	**Gal2**	**Glc**
H1-H3	-	2.7 / **2.4**	2.6 / **2.0**	2.7 / **2.2**	2.7
H3-H5	2.6 / **2.6**	2.5	2.7	2.5	2.6
LSTc	**Neu5Ac(*)**	**Gal1**	**GlcNAc**	**Gal2**	**Glc**
H1-H3	-	2.7 / **2.1**	2.6 / **2.1**	2.7 / **2.5**	2.7
H3-H5	2.6 **/ 2.3**	2.54	2.6	2.5	2.7

Average value of distances H1-H3 and or H3-H5 for each residue calculated on 100 ns MD simulation. In bold face the corresponding experimental distances are reported as obtained by the NOESY extrapolated at short mixing time. (*) For Neu5Ac the considered distances is the H3ax-H5. An estimate of the errors on each distance value is reported in brackets on the last decimal digit.

Supplementary Table 4. *Comparison between measured and simulated (NOEPROM) inter-residue proton-proton percentage NOE signals (%NOE).*Percentage NOEs were simulated for the RMSD$_{exp}$ min and max groups for LSTc and LSTa, and of the last 60 conformers of the MD simulation (calc.), mixing times (Tm) span 0.1 to 0.8 s. All NOEs were measured at 900 MHz apart from CH_3GlcNAc:H5-Neu5Ac for LSTc which was measured at 600 MHz.

		LSTc				LSTa	
CH_3GlcNAc		**H5Neu5Ac**		**H3Gal1**		**H3axNeu5Ac**	
Tm(s)	**Exp. / Calc.**	**RMSD$_{exp}$ min**	**RMSD$_{exp}$ max**	**Tm (s)**	**Exp. / Calc.**	**RMSD$_{exp}$ min**	**RMSD$_{exp}$ max**
0.1	0.07 / 0.00	0.04	0.00	**0.20**	1.26 / 0.00	2.10	0.10
0.2	0.10 / 0.00	0.09	0.00	**0.30**	1.12 / 0.00	3.20	0.20
0.3	0.14 / 0.00	0.13	0.00	**0.50**	1.55 / 0.00	5.40	0.30
0.5	0.19 / 0.00	0.23	0.00	**0.80**	2.21 / 0.00	8.90	0.50
0.7	0.23 / 0.00	0.32	0.00				
						RMSD$_{exp}$ min (ϕ_1/ψ_1)	
						-99.5°/-52.9°	**206.6°/-23.8°**
				0.20	1.26 / 0.00	0.41	4.10
				0.30	1.12 / 0.00	0.63	6.30
				0.50	1.55 / 0.00	1.10	10.6
				0.80	2.21 / 0.00	1.8	17.9
H1Gal1		**H4GlcNAc**		**H1Gal1**		**H3GlcNAc**	
0.15	3.80 / 3.92	3.60	0.80	**0.20**	4.44 / 4.56	5.20	1.90
0.2	5.20 / 5.20	4.80	1.00	**0.30**	6.09 / 6.83	7.80	2.90
0.3	6.80 / 7.80	7.30	1.5	**0.50**	11.07 / 11.39	13.10	4.80
				0.80	18.18 / 18.22	20.90	7.70
H1GlcNAc		**H3Gal2**		**H1GlcNAc**		**H3Gal2**	
0.1	1.16 / 2.21	1.40	1.90	**0.20**	5.15 / 3.9	7.20	0.70
0.2	2.40 / 4.43	2.70	3.70	**0.30**	7.73 / 5.85	10.80	1.00
0.3	3.50 / 6.65	4.10	5.60	**0.50**	12.98 / 9.81	18.00	1.70
0.5	7.30 / 11.20	6.80	9.30	**0.80**	19.91 / 15.79	28.80	2.80
0.8	9.90 / 18.00	11.00	14.90				
H1Gal2		**H4Glc**		**H1Gal2**		**H4Glc**	
0.15	2.40 / 3.50	2.80	2.50	**0.20**	3.80 / 4.98	5.70	5.20
0.2	2.60 / 4.66	3.70	3.30	**0.30**	5.90 / 7.47	8.60	7.80
0.3	3.40 / 7.01	5.50	5.00	**0.50**	10.30 / 12.45	14.30	13.00
				0.80	22.30 / 19.93	23.00	20.90

Supplementary Table 5. Torsional states of LSTa and LSTc conformers selected by $RMSD_{exp}$ analysis

LSTa (α2→3) Torsional angles

	linkage	ϕ	ψ
RMSDmin	1	-100	-53
		207	-24
	2	41	-1
	3	27	-36
	4	38	-5
RMSDmax	1	-58	-10
	2	62	45
		-31	-20
	3	60	55
	4	38	-2

LSTc (α2→6) Torsional angles

	linkage	ϕ	ψ
RMSDmin	1	-55	197
	2	28	-15
	3	34	-53
	4	11	-15
RMSDmax	1	64	185
		-64	144
	2	-54	-42
		43	22
	3	18	-41
		35	37
	4	29	-11

Supplementary Table 6. LSTc and LSTa hydrogen bond networks.

LSTc (α2→6) proposed hydrogen bonds that are present in greater than 10% of the selected conformers (Neu5Ac-α(2→6)-Gal-β(1→4)-GlcNAc-β(1→3)-Gal-β(1→4)-Glc).

	From	Residue	To	Residue	%
RMSDmin	H3O	GlcNAc	O5	Gal1	100.0
	H4O	Gal2	O5	GlcNAc	82.5
	H3O	Glc	O5	Gal2	62.5
	O3	GlcNAc	H7O	NeuAc	55.0
	H2O	Gal2	O2N	GlcNAc	42.5
	H3O	GlcNAc	O6	Gal1	25.0
	O5	Gal1	H8O	NeuAc	20.0
	H2N	GlcNAc	O5N	NeuAc	15.0
	H3O	Glc	O6	Gal2	12.5
	H3O	GlcNAc	O6	NeuAc	12.5
	H2N	GlcNAc	O7	NeuAc	12.5
RMDSmax	H3O	Glc	O5	Gal2	82.5
	H2O	Gal2	O2N	GlcNAc	30.0
	H3O	Glc	O6	Gal2	17.5
	H4O	Gal2	O5	GlcNAc	15.0
	H6O	Glc	O2	Gal2	12.5
	O3	GlcNAc	H2O	Gal1	10.0

LSTa (α2→3) proposed hydrogen bonds that are present in greater than 10% of the selected conformers (Neu5Ac-α(2→3)-Gal-β(1→3)-GlcNAc-β(1→3)-Gal-β(1→4)-Glc).

	From	Residue	To	Residue	%
RMSD min	H4O	GlcNAc	O5	Gal1	92.5
	H3O	Glc	O5	Gal2	80.0
	H4O	Gal1	O1B	NeuAc	42.5
	H4O	Gal2	O5	GlcNAc	22.5
	H4O	Gal1	O1A	NeuAc	10.0
RMSD max	H3O	Glc	O5	Gal2	85.0
	H2O	Gal1	O6	NeuAc	52.5
	H4O	Gal2	O2N	GlcNAc	35.0
	H2N	GlcNAc	O5	Gal1	25.0
	H4O	GlcNAc	O5	Gal1	17.5
	O2	Gal1	H8O	NeuAc	17.5
	H3O	Glc	O6	Gal2	15.0
	H2N	GlcNAc	O2	Gal1	10.0

Supplementary Table 7. *Experimental and calculated $^3J_{CH}$ interglycosidic coupling constants (Hz) for LSTa and LSTc (Jϕ = H1-C1-O-Cx and Jψ = C1-O-Cx-Hx).* The corresponding calculated value are done using the $RMSD_{exp}$ min sets and the Karplus type equation reported by (Tvaroska I., et al. , M. (1989) Carbohydrate Res., 189, 359-362).

LSTa	$J^{exp}\phi$ (Hz)	$J^{calc}\phi$ (Hz)	$J^{exp}\psi$ (Hz)	$J^{calc}\psi$ (Hz)
Neu5Ac-Gal1 (ϕ_1/ψ_1)	-	-	4.4	2.2 (ϕ_1/ψ_1 = -99°/-53°)
				4.7 (ϕ_1/ψ_1 = 207°/-24°)
Gal1-GlcNAc (ϕ_2/ψ_2)	2.6	3.7	5.4	5.5
GlcNAc-Gal2 (ϕ_3/ψ_3)	4.2	4.8	4.5	3.8
Gal2-Glc (ϕ_4/ψ_4)	4.1	3.8	-	5.6
LSTc				
Neu5Ac-Gal1 (ϕ_1/ψ_1)	-	-	2.6	4.0
Gal1-GlcNAc (ϕ_2/ψ_2)	3.6	4.4	-	5.3
GlcNAc-Gal2 (ϕ_3/ψ_3)	4.1	3.9	4.4	2.2
Gal2-Glc (ϕ_4/ψ_4)	3.4	3.5 (ϕ_4/ψ_4 = 39°/-7°)	-	5.5 (ϕ_4/ψ_4 = 39°/-7°)
		3.7 (ϕ_4/ψ_4 = -36°/-30°)		4.3 (ϕ_4/ψ_4 = -36°/-30°)

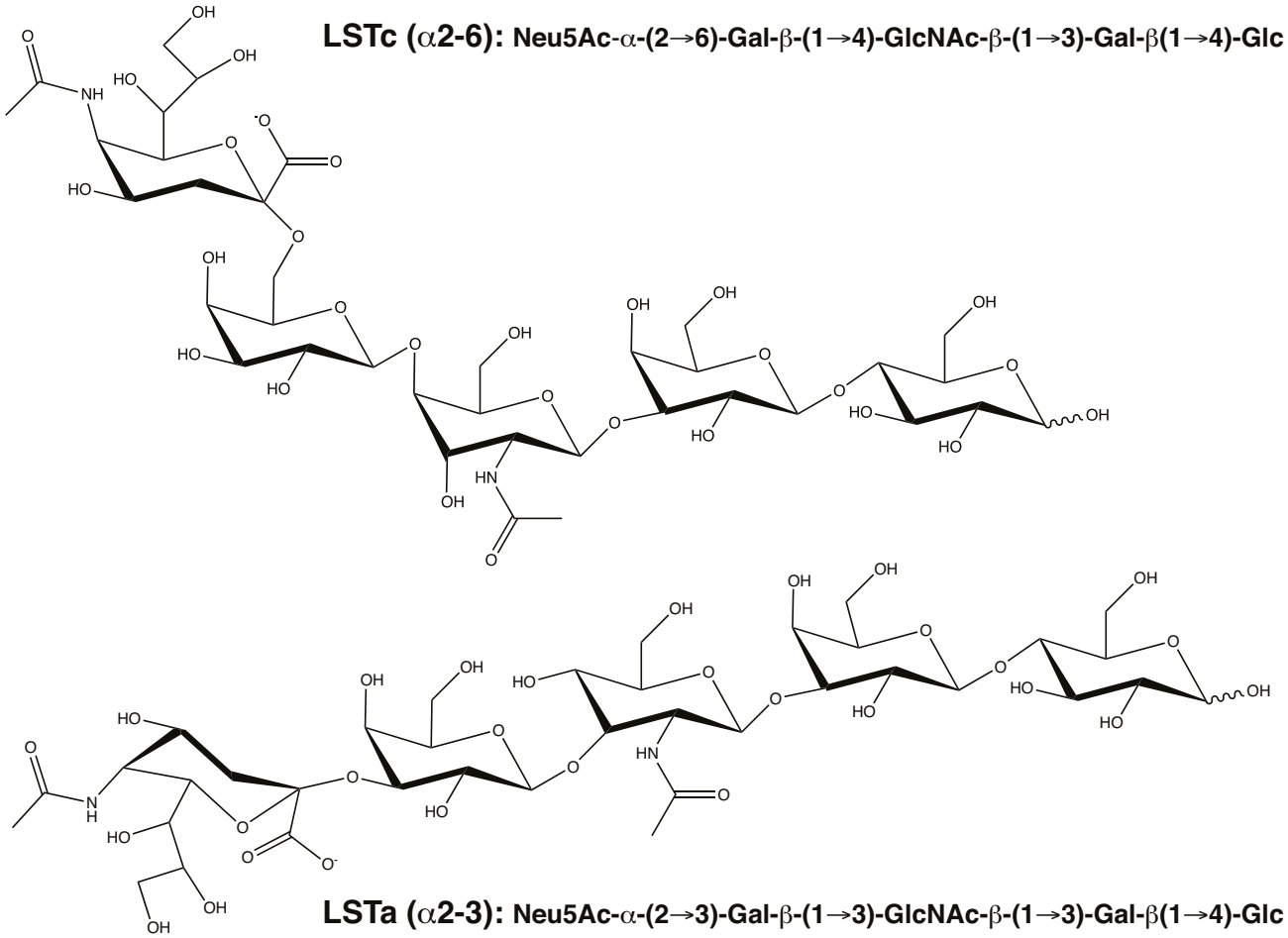

Supplementary Figure 1. Scheme of human milk lactosyl sialyl-N-tetraoses.

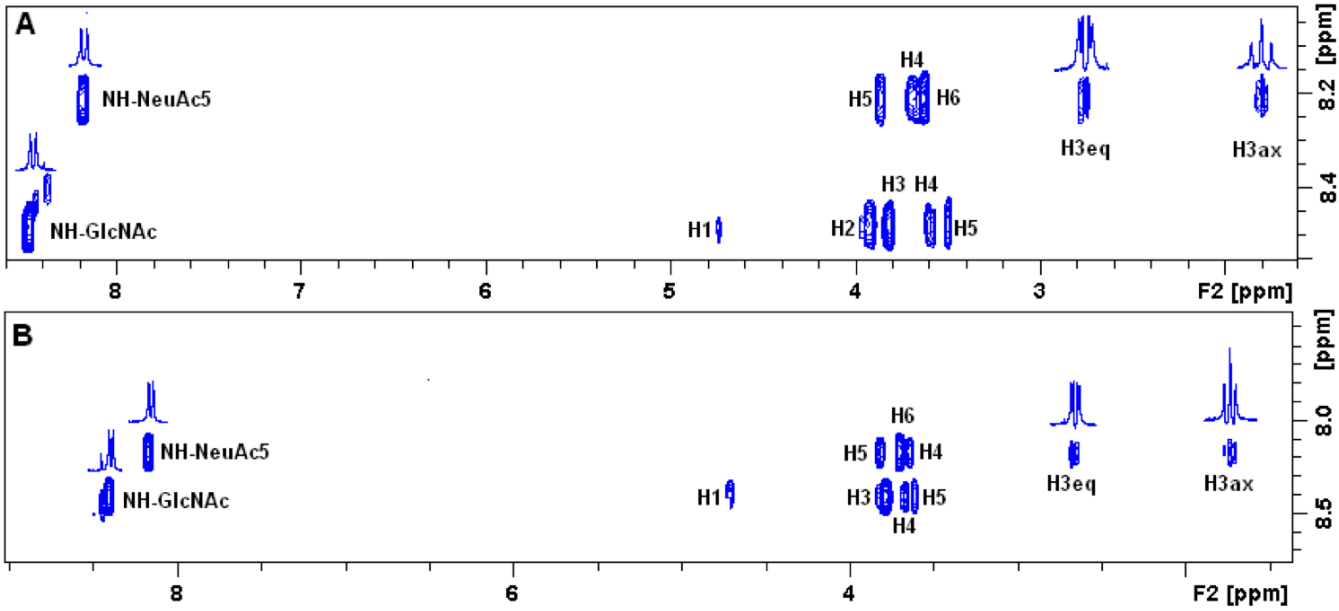

Supplementary Figure 2. 2D Partial TOCSY spectra of NH coupling spin systems from Neu5Ac and GlcNAc at 278 K, buffered system containing 10% D_2O, pH 7.2. (A) LSTa and (B) LSTc.

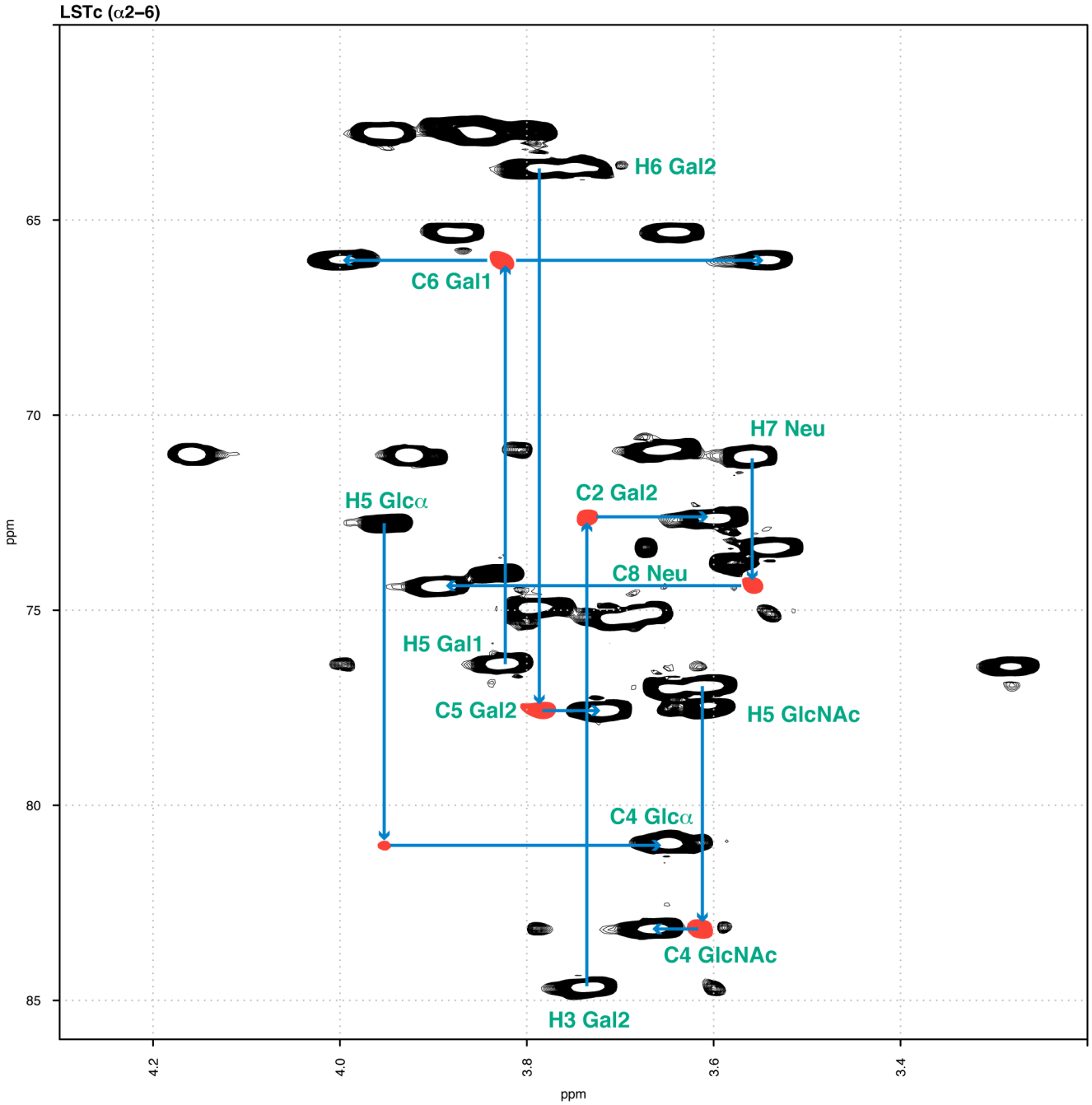

Supplementary Figure 3. Example of signal assignment of a sensitivity-enhanced HSQC spectrum using cross peaks generated by homonuclear proton coupling.

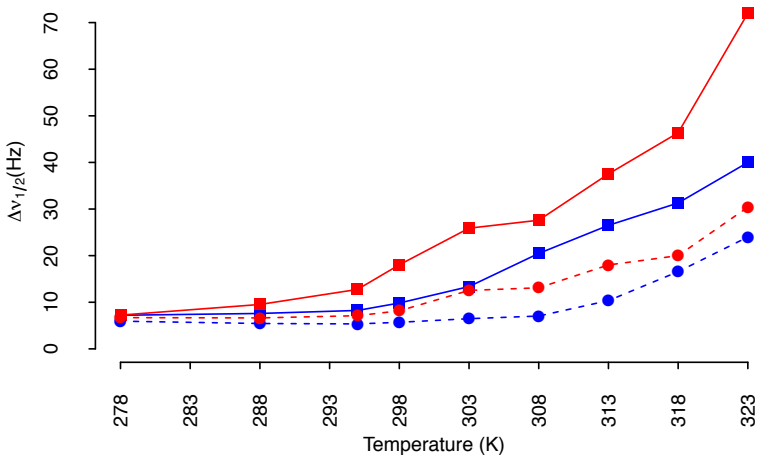

Supplementary Figure 4. Experimental curves of NH $\Delta\upsilon_{½}$ [Hz] plotted against temperature [K]. LSTc (square), LSTa (circle), Neu5Ac (red), GlcNac (blue).

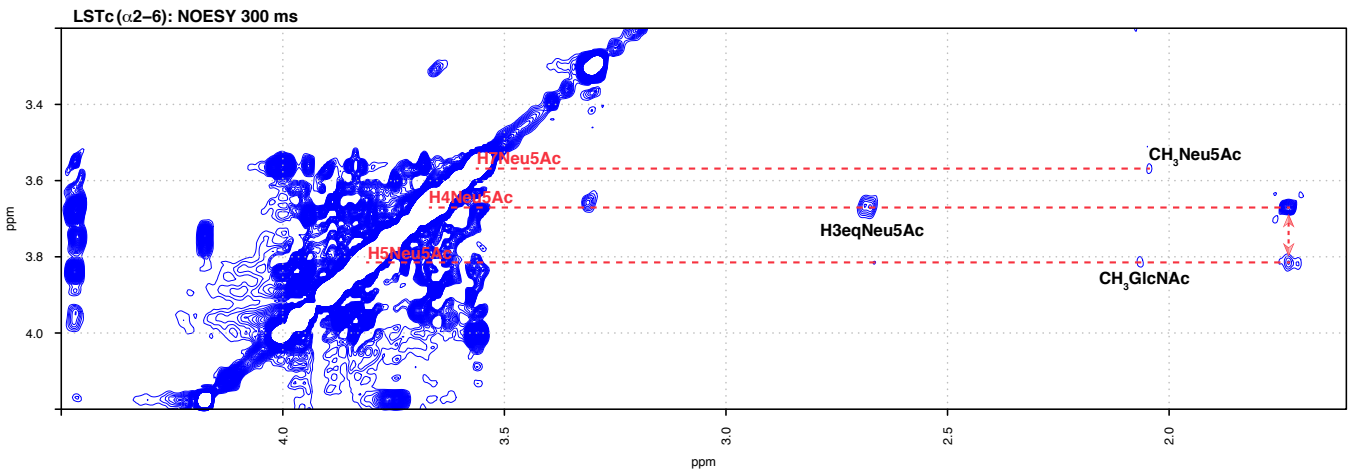

Supplementary Figure 5. 2D Partial NOESY (300 ms at 295 K) spectrum of LSTc showing the inter-residue NOE contact of H5Neu5Ac and CH_3GlcNAc and the intra-residue NOE contacts of H4-, H5- and H7-Neu5Ac in the diagonal line.

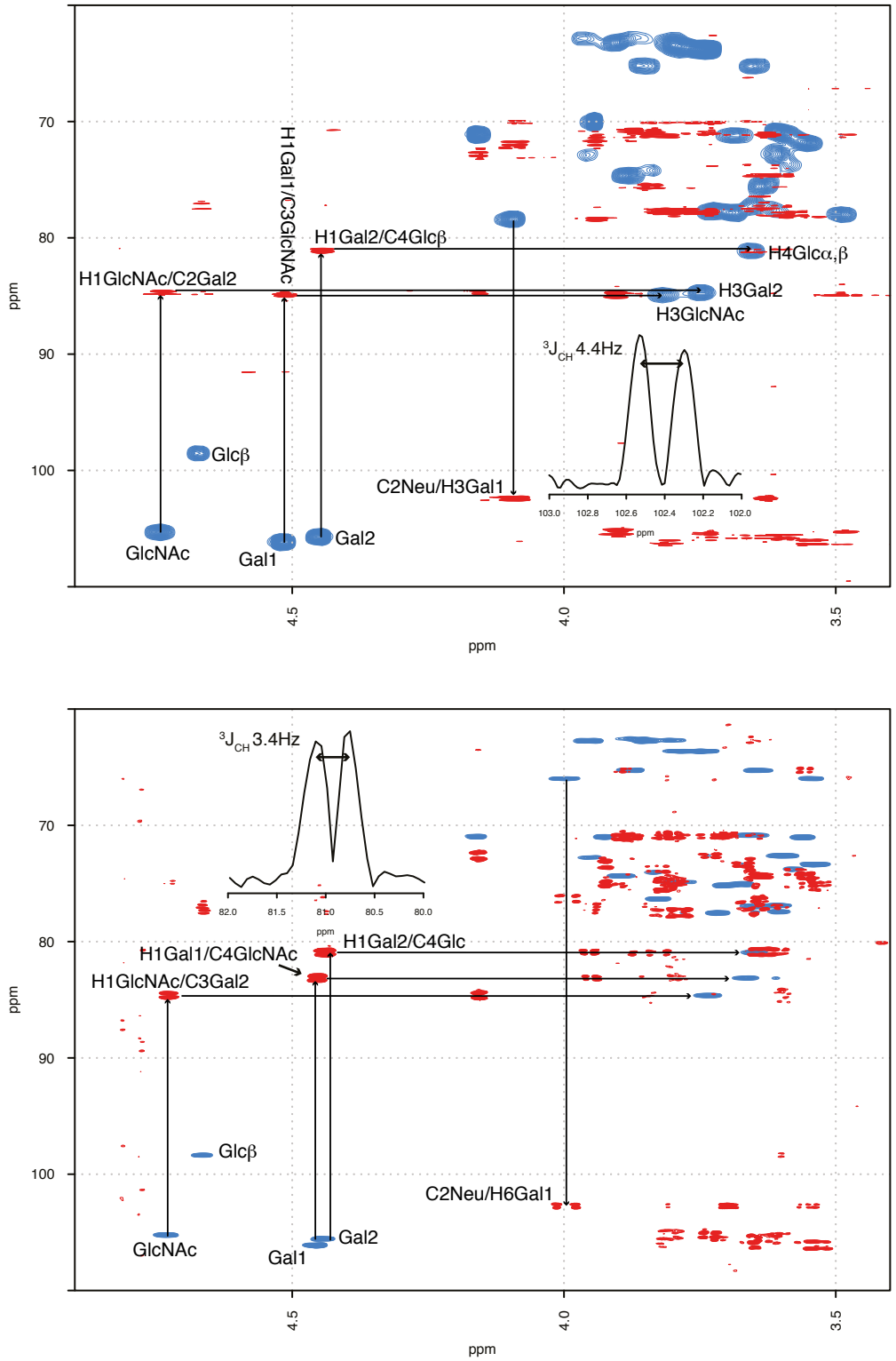

Supplementary Figure 6. J-HMBC (red) and HSQC (blue) spectra of LSTa (top) and LSTc (bottom). The 1D-J-HMBC slice extracted for LSTa is the long range coupling for C2Neu/H3Gal1, while the 1D-J-HMBC slice shown for LSTc is the long range coupling for H1Gal2/C5Glc.

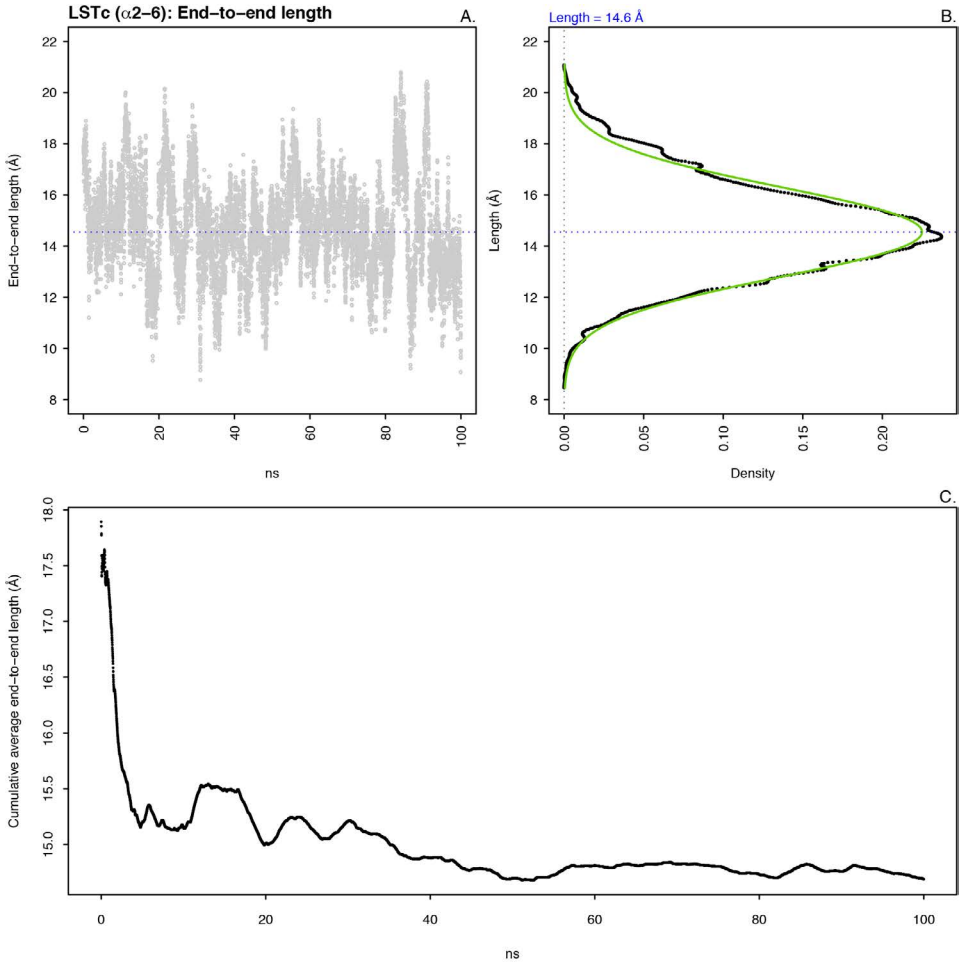

Supplementary Figure 7. *End-to-End length analysis of LSTc over the MD simulation, 100 ns, 295 K.* **A**. end-to-end length, **B**., density plot of the end-to-end lengths and **C**. cumulative average end-to-end length.

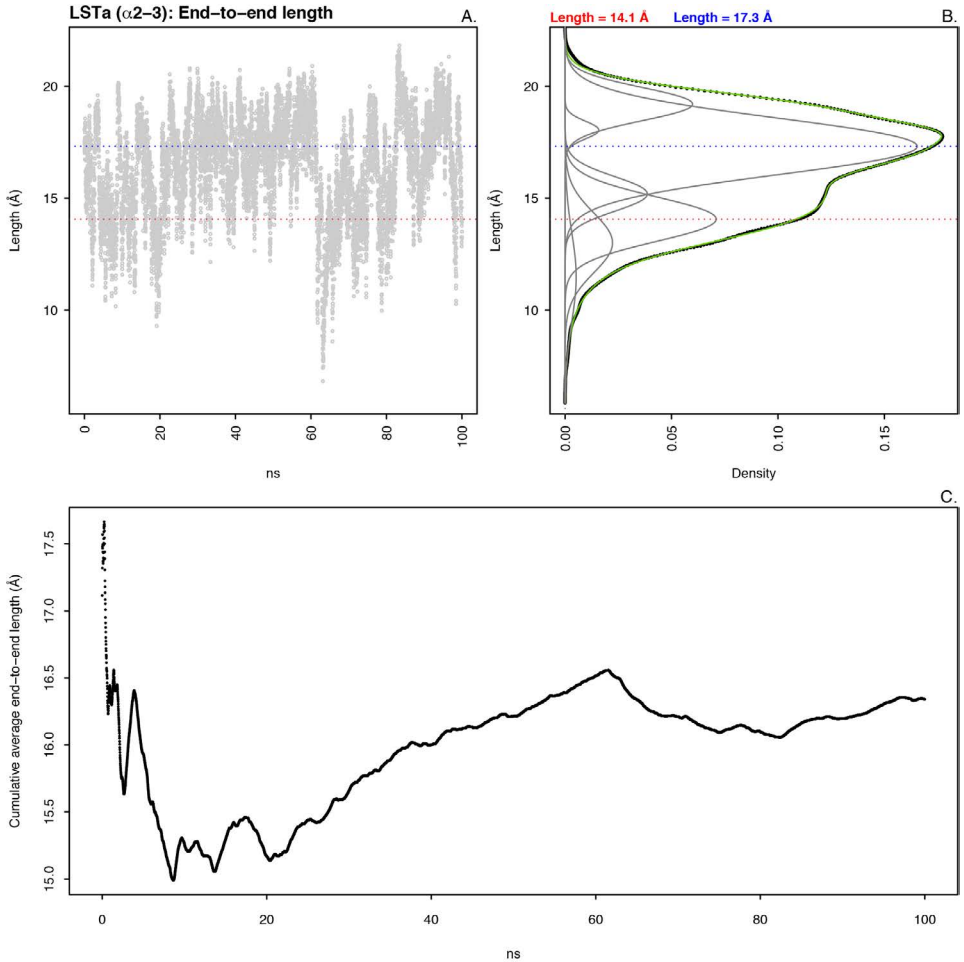

Supplementary Figure 8. *End-to-End length analysis of LSTa over the MD simulation, 100 ns, 295 K.* **A**. end-to-end length, **B**., density plot of the end-to-end lengths and **C**. cumulative average end-to-end length.

The end-to-end distance is one of the slowest time evolving molecular properties for oligomers, for LSTc and LSTa this distance is defined as the distance between the non-reducing end Neu5Ac C5 and the reducing end Glc C4. For both LSTc and LSTa this property exhibits stationarybehaviour after 50-70 ns.

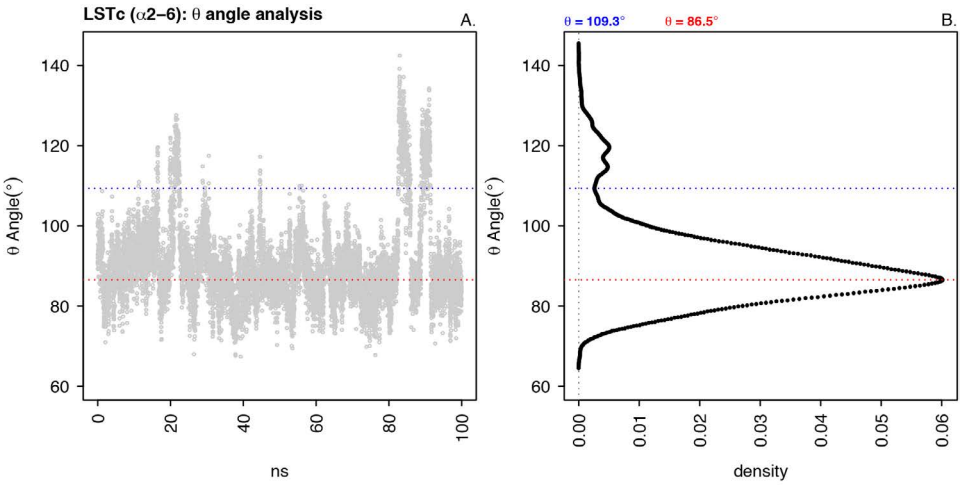

Supplementary Figure 9. *LSTc θ angle*. **A.** θ angle, **B.** density of θ angle.

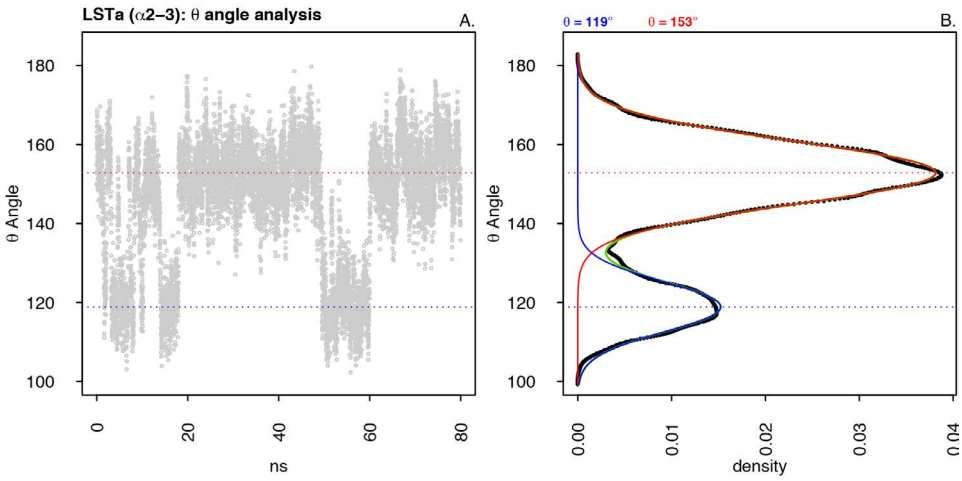

Supplementary Figure 10. *LSTa θ angle*. **A.** θ angle, **B.** density of θ angle.

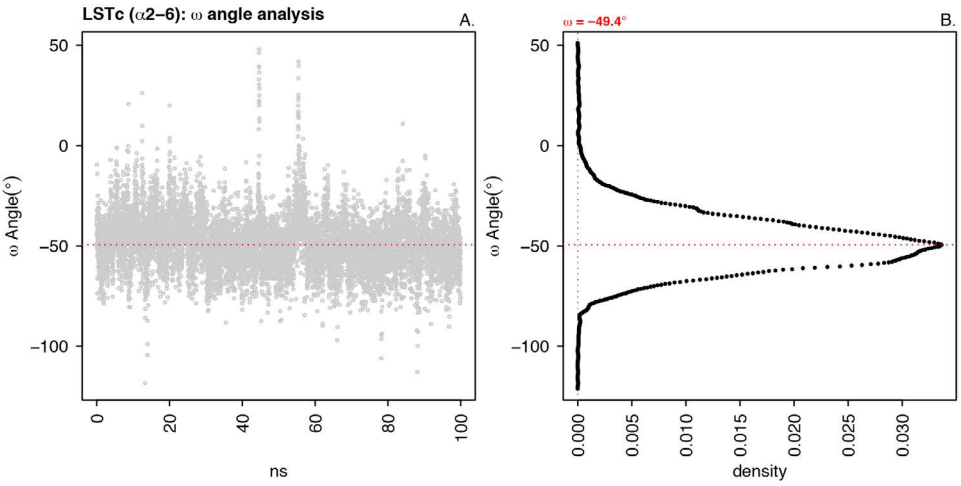

Supplementary Figure 11. *LSTc ω angle*. **A.** ω angle, **B.** density of ω angle.

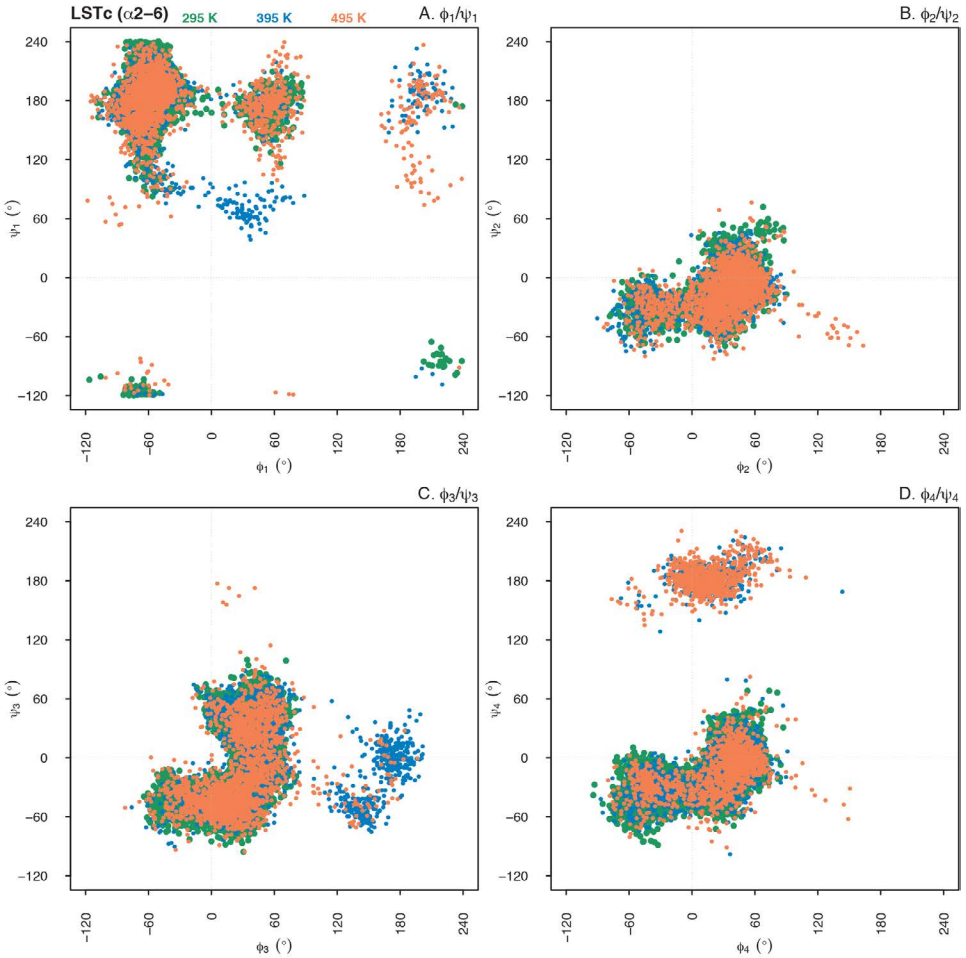

Supplementary Figure 12. *Glycosidic torsionals angles of LSTc at 295, 395 and 495 K.* At 295 K the MD simulation length was 100 ns, while at 395 and 495 K it was 20 ns.

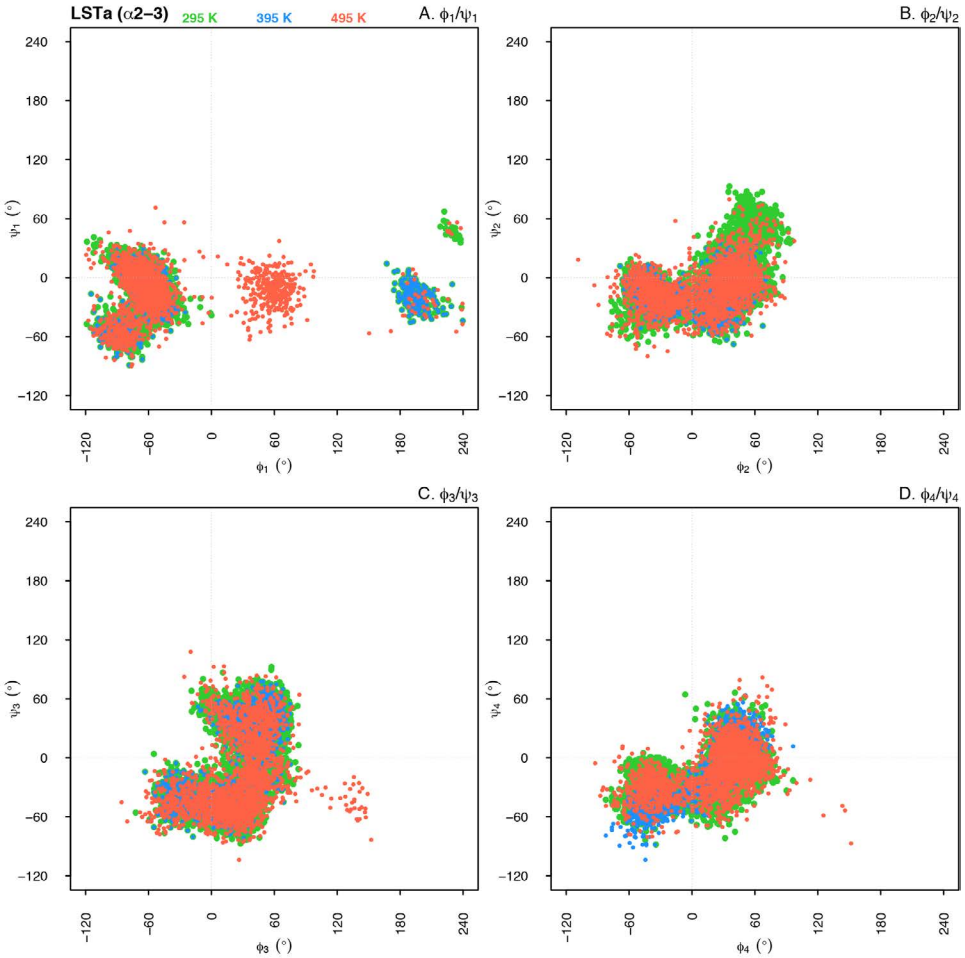

Supplementary Figure 13. *Glycosidic torsionals angles of LSTa at 295, 395 and 495 K.* At 295 K the MD simulation length was 100 ns, while at 395 and 495 K it was 20 ns.

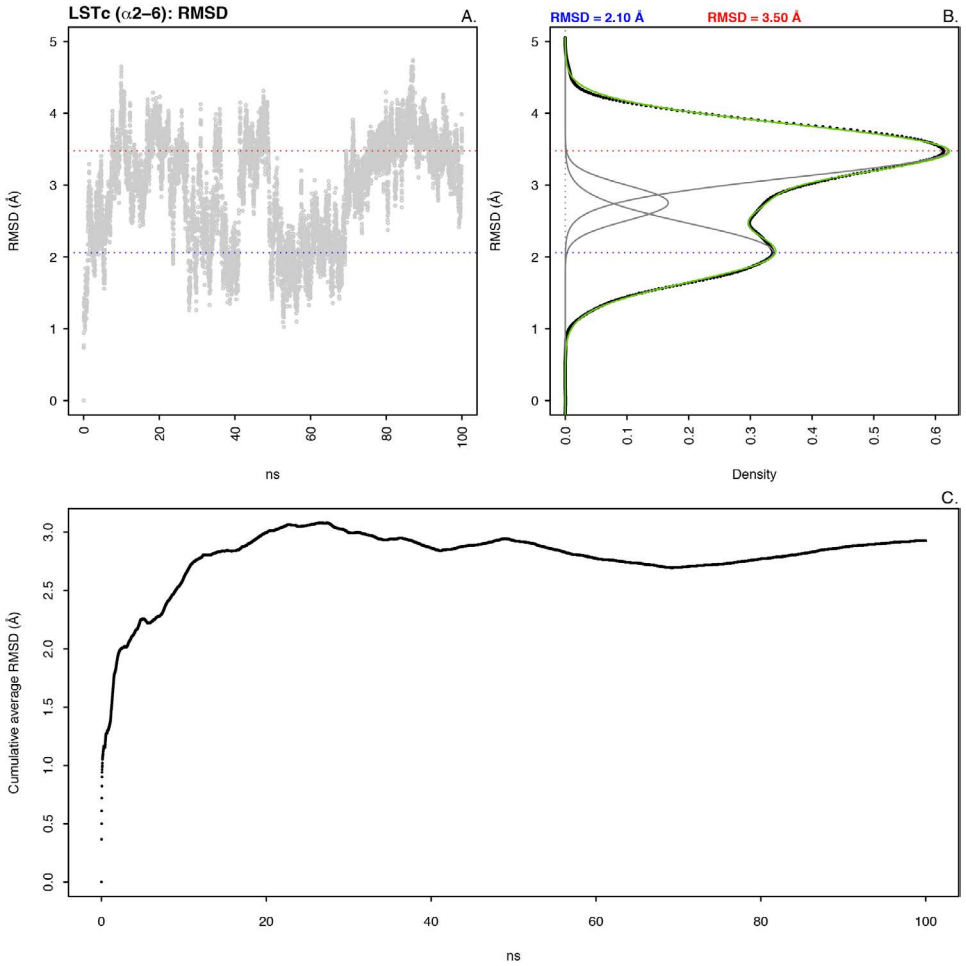

Supplementary Figure 14. *RMSD analysis of LSTc over the MD simulation, 100 ns, 295 K.* **A**. RMSD, **B**. density plot of the RMSD and **C**. cumulative average RMSD.

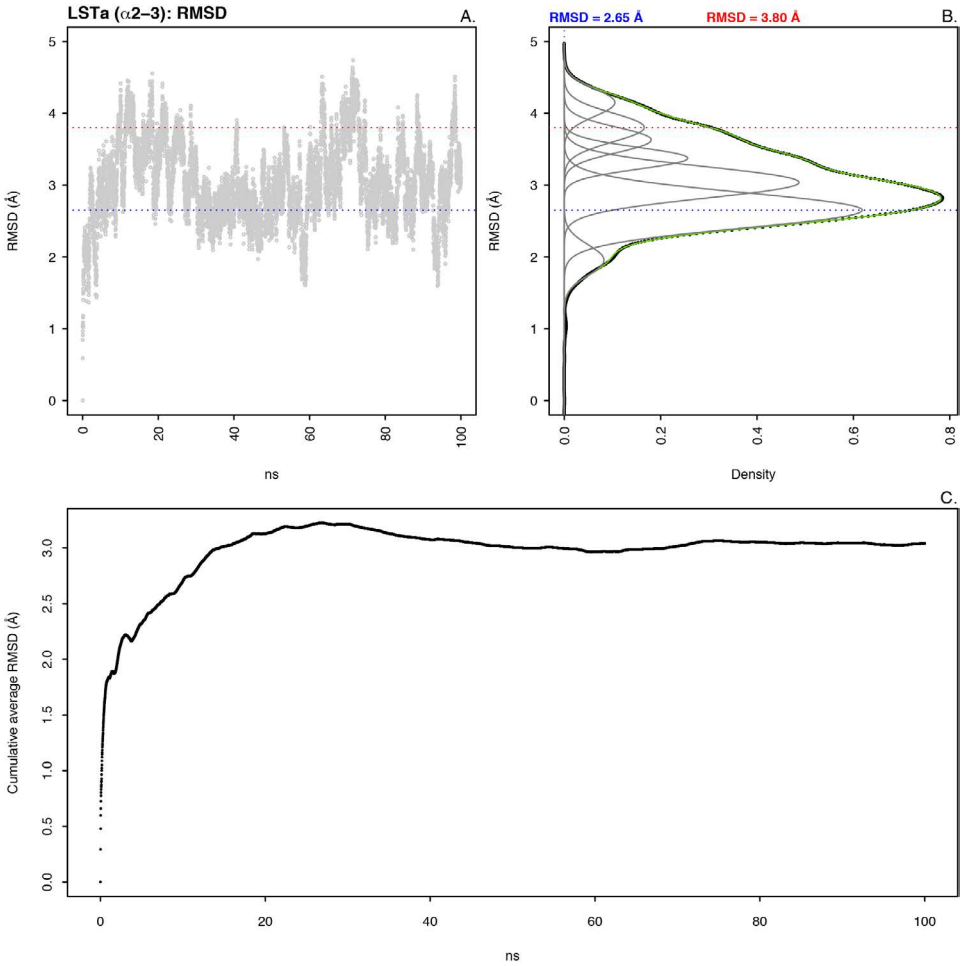

Supplementary Figure 15. *RMSD analysis of LSTa over the MD simulation, 100 ns, 295 K.* **A**. RMSD, **B**. density plot of the RMSD and **C**. cumulative average RMSD.

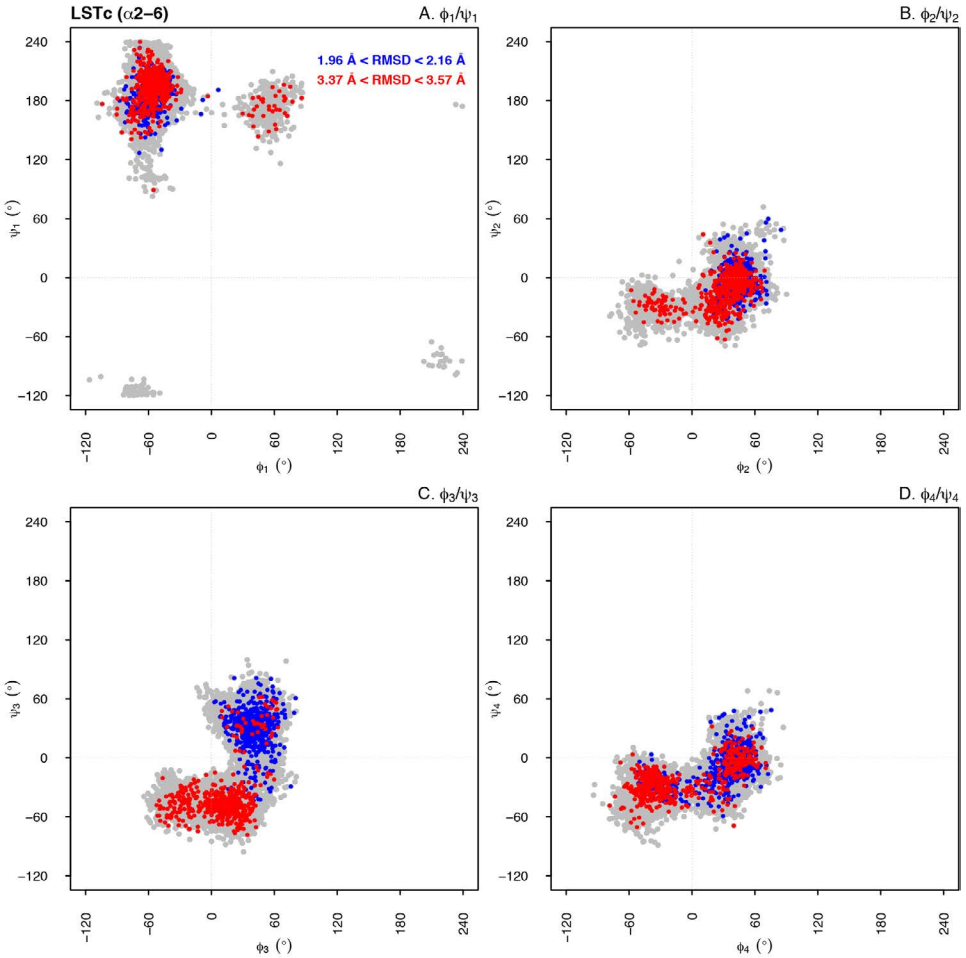

Supplementary Figure 16. *Glycosidic torsionals angles of LSTc with conformers from the different RMSD populations highlighted (blue -1.96 Å < RMSD < 2.16* Å and red - *3.37 Å < RMSD < 3.57* Å).

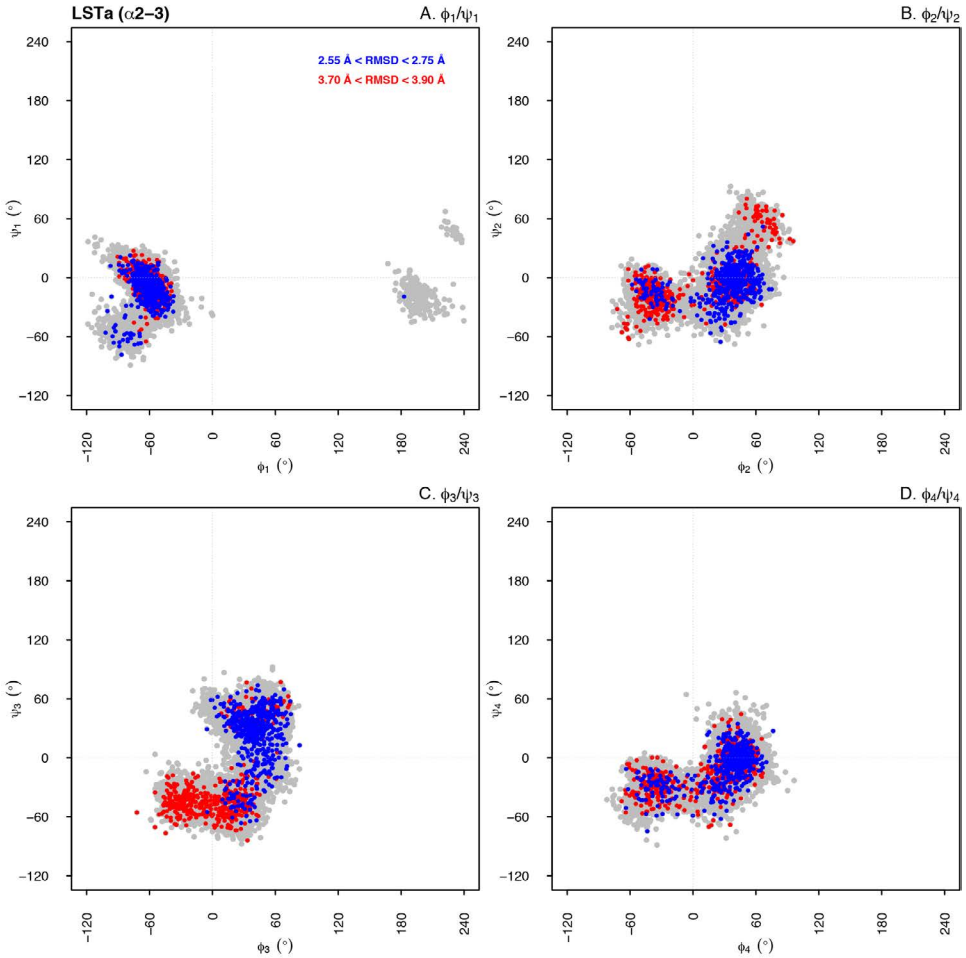

Supplementary Figure 17. *Glycosidic torsionals angles of LSTa with conformers from the different RMSD populations highlighted (blue - 2.55 Å < RMSD < 2.75 Å and red - 3.70 Å < RMSD < 3.90 Å).*

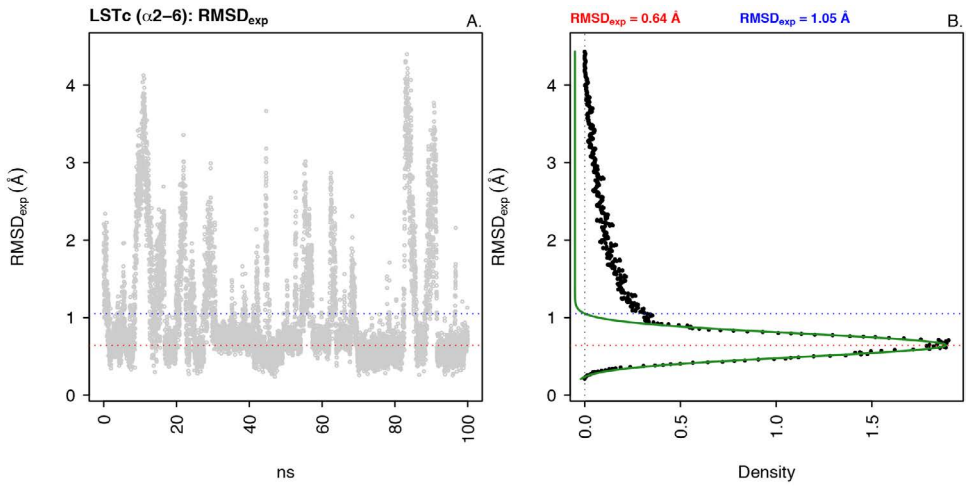

Supplementary Figure 18. *LSTc RMSD$_{exp}$ analysis*. **A.** RMSD$_{exp}$, **B.** RMSDexp density.

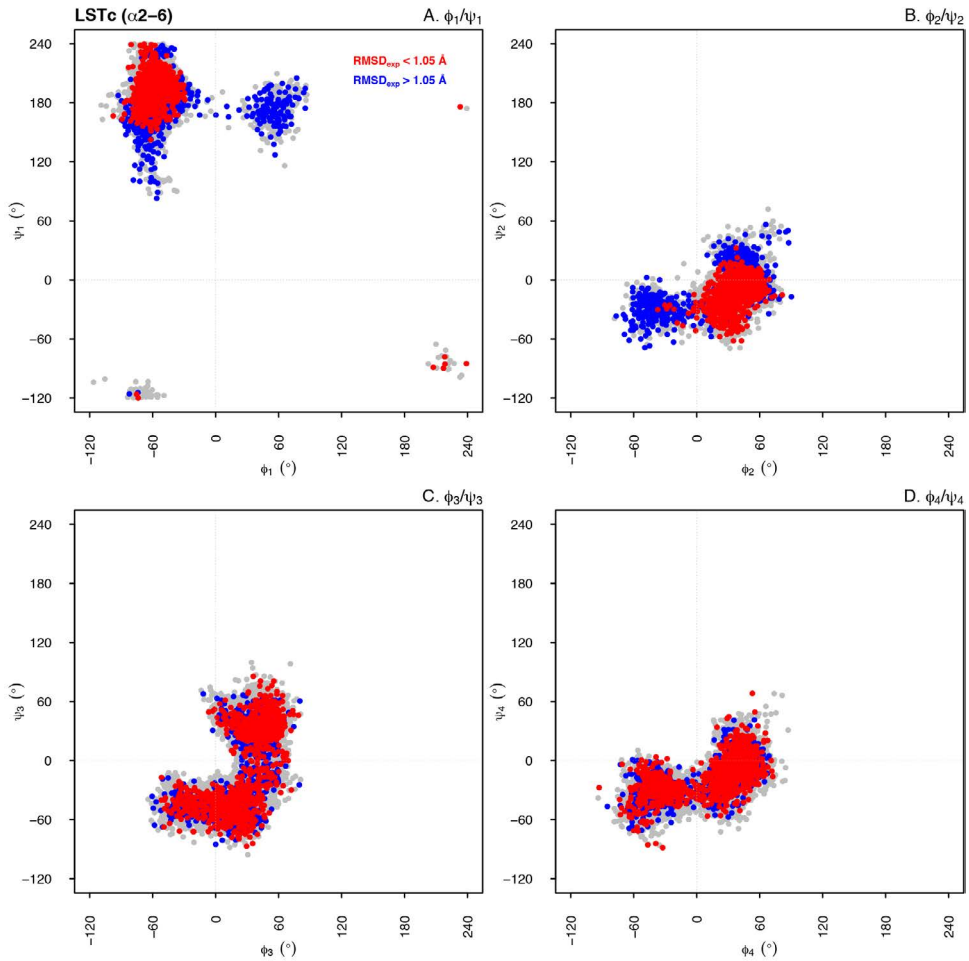

Supplementary Figure 19. *Glycosidic torsionals angles of LSTc* . The red dots correspond to a subset of conformers with a RMSD$_{exp}$ < 1.05 Å, while the blue dots correspond to a subset of conformers with a RMSD$_{exp}$ > 1.05 Å.

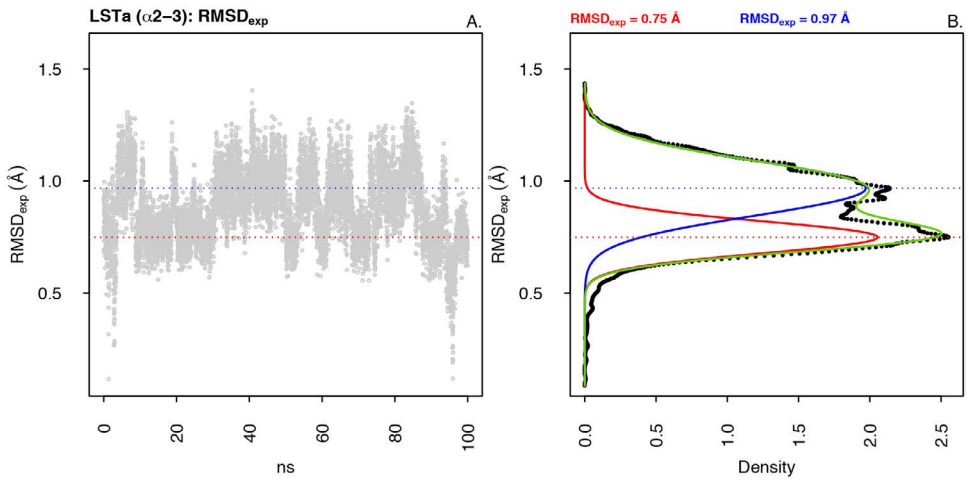

Supplementary Figure 20. *LSTa $RMSD_{exp}$ analysis*. **A.** $RMSD_{exp}$, **B.** $RMSD_{exp}$ density.

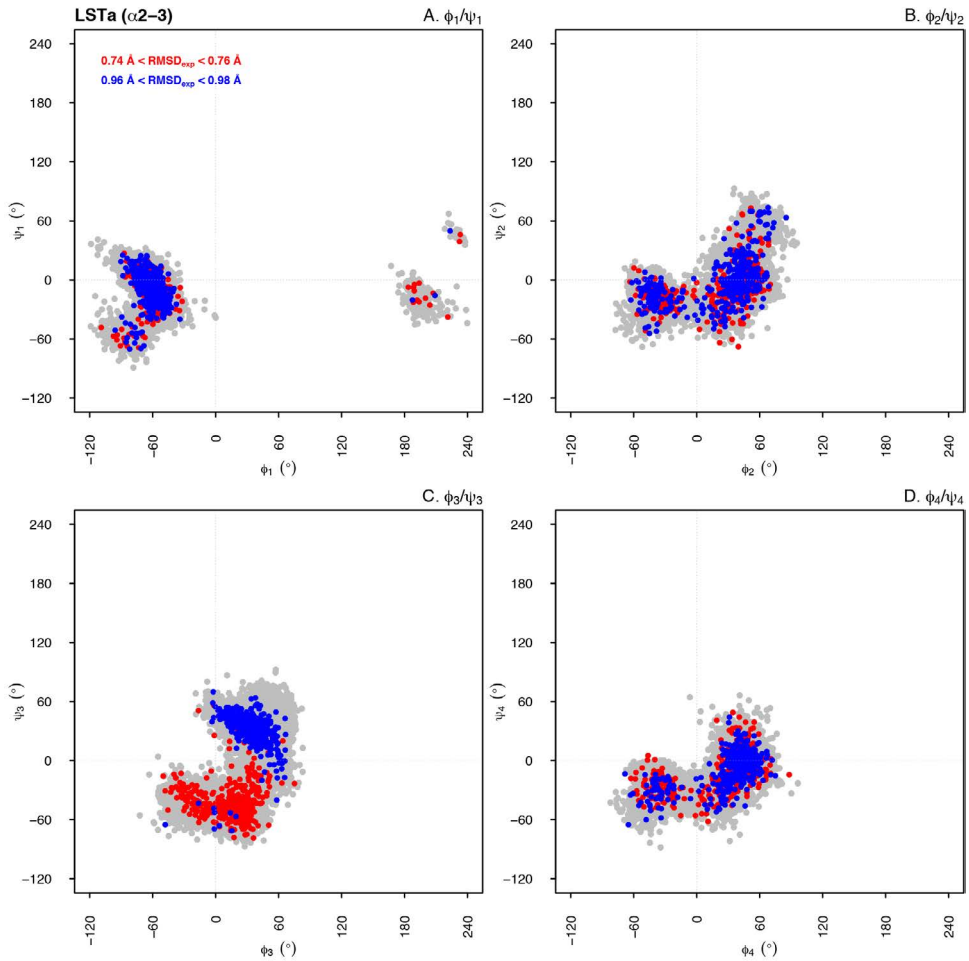

Supplementary Figure 21. *Glycosidic torsionals angles of LSTa*. The red dots correspond to a subset of conformers in the range 0.74 Å < $RMSD_{exp}$ < 0.76 Å, while the blue dots correspond to a subset of conformers in the range 0.96 Å < $RMSD_{exp}$ < 0.98 Å.

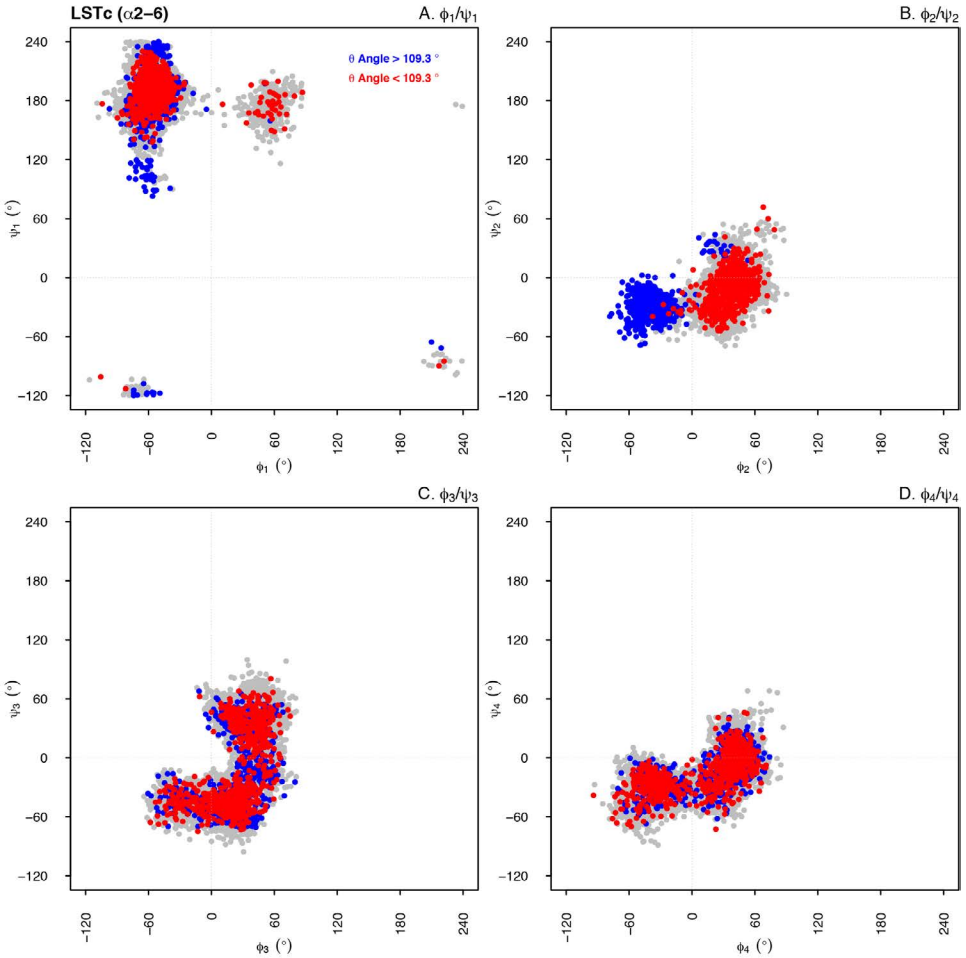

Supplementary Figure 22. *Glycosidic torsionals angles of LSTc* . The red dots correspond to a subset of conformers with a θ angle < 109.3°, while the blue dots correspond to a subset of conformers with a θ angle >109.3°.

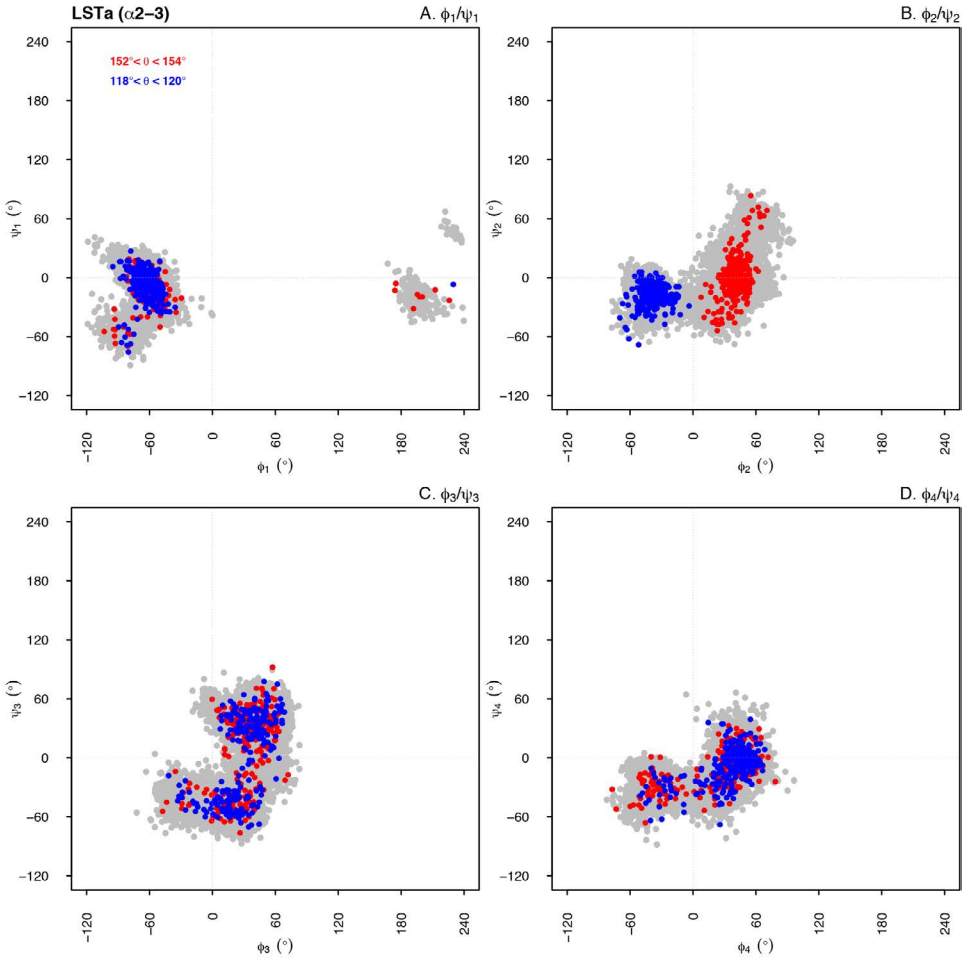

Supplementary Figure 23. *Glycosidic torsionals angles of LSTa*. The red dots correspond toa subset of conformers in the range 152° < θ angle < 154° , while the blue dots correspond to a subset of conformers with the range 118° < θ angle < 120°.

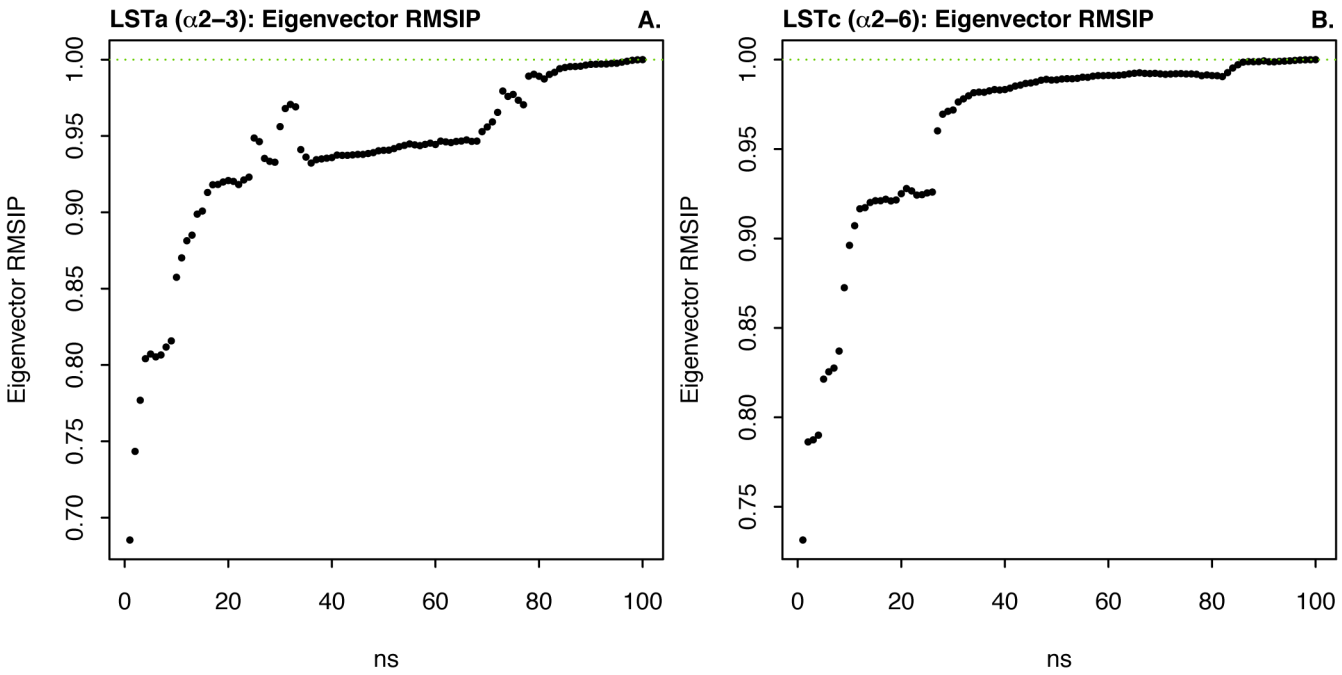

Supplementary Figure 24. *RMSIP analysis of the eigenvectors (first ten) derived by PCA of the LSTa (***A.***) and LSTc (***B.***) MD simulation.*

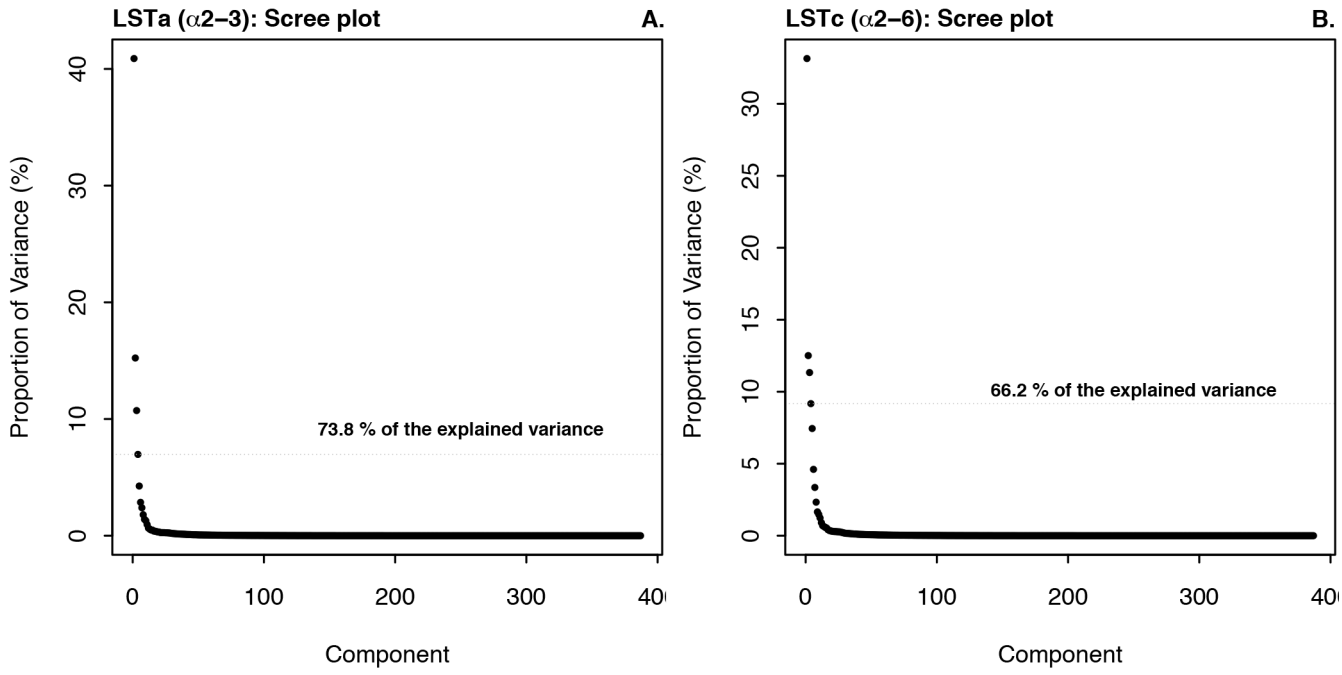

Supplementary Figure 25. *PCA Scree plots for the analysis of the LSTa (***A.***) and LSTc (***B.***) MD simulation.*

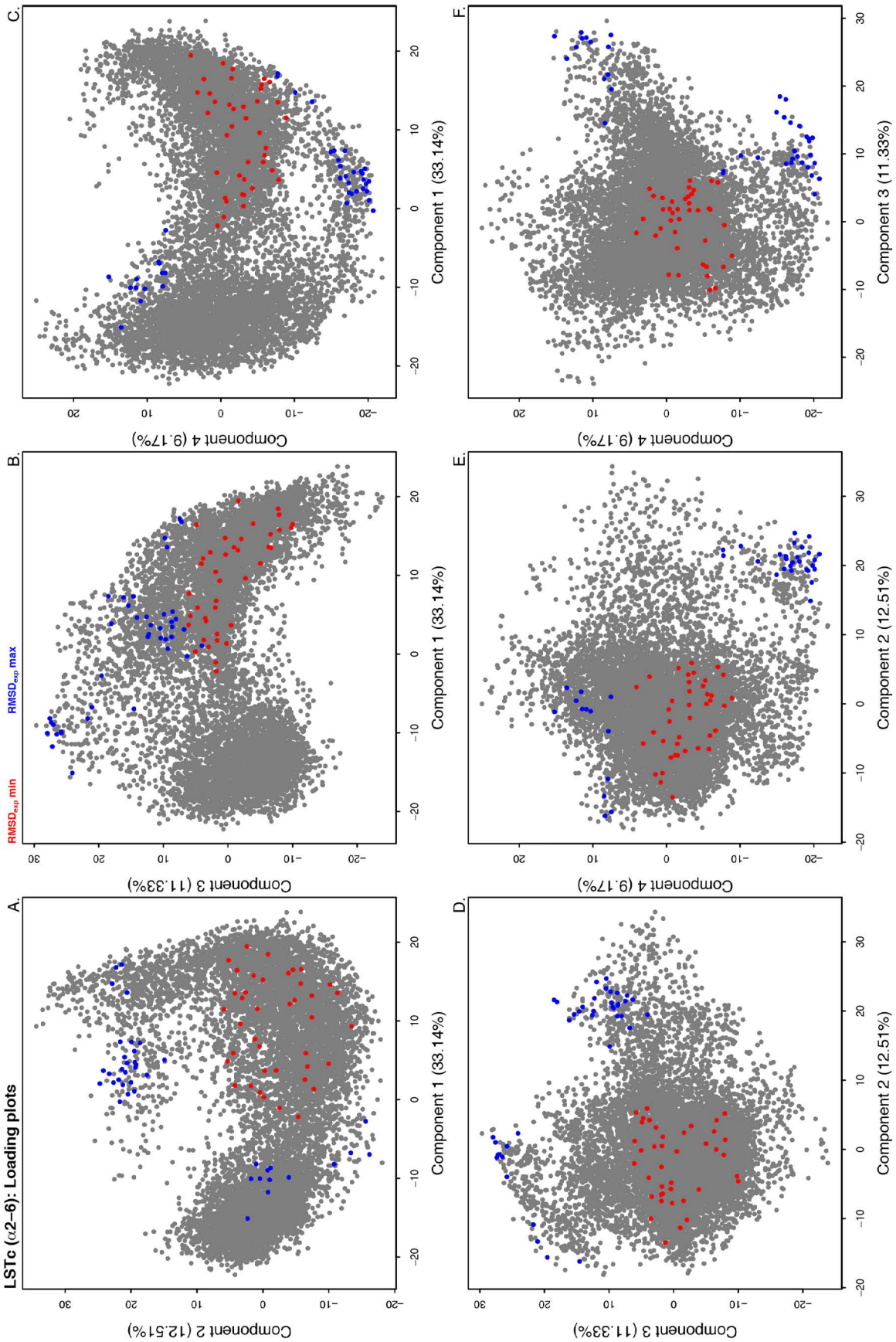

Supplementary Figure 26. *PCA Loading plot for the analysis of the LSTc MD simulation.* The red dots correspond to the $RMSD_{exp}$ min conformers, while the blue dots correspond to the $RMSD_{exp}$ max conformers.

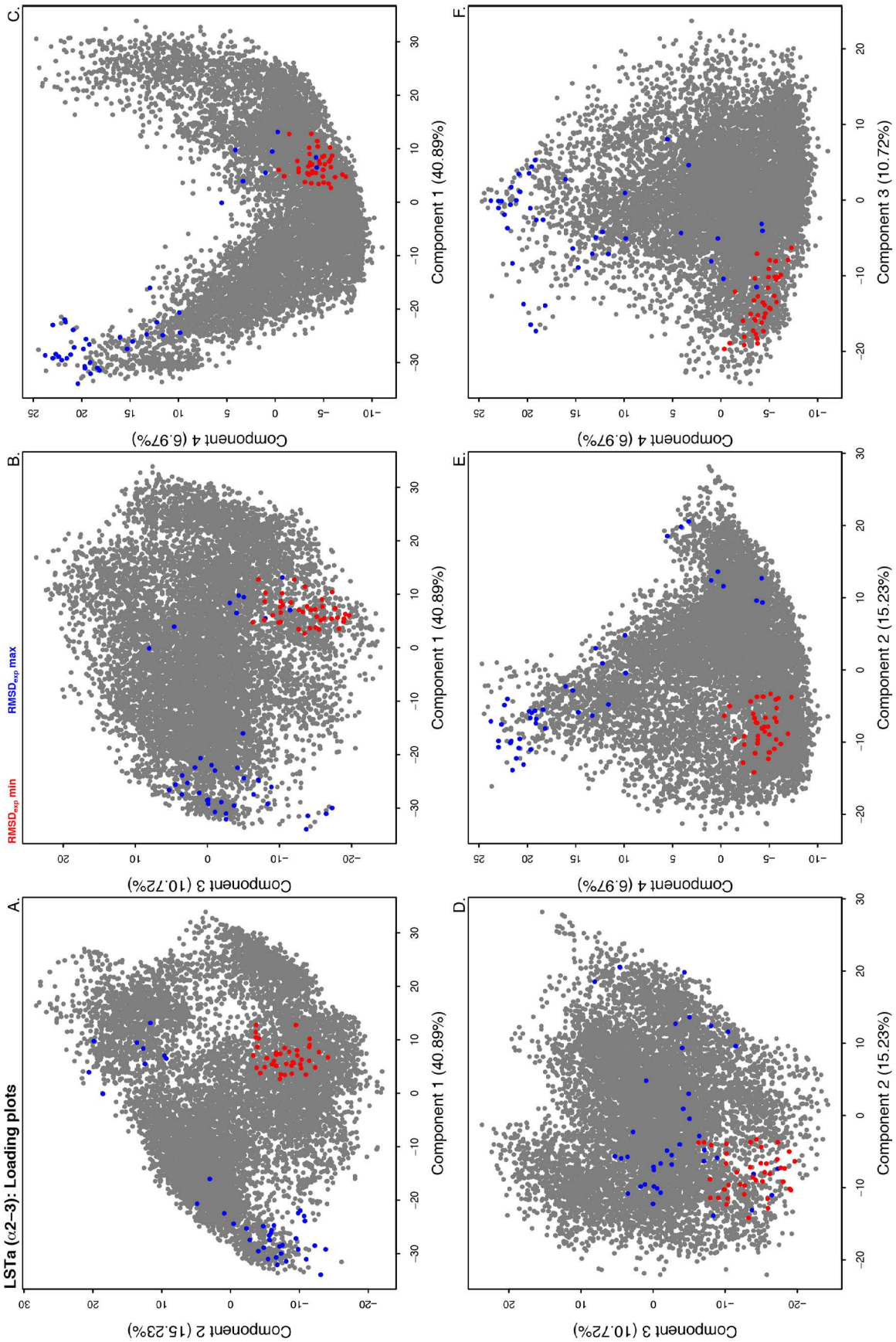

Supplementary Figure 27. *PCA Loading plot for the analysis of the LSTa MD simulation.* The red dots correspond to the RMSDexp min conformers, while the blue dots correspond to the RMSDexp max conformers.

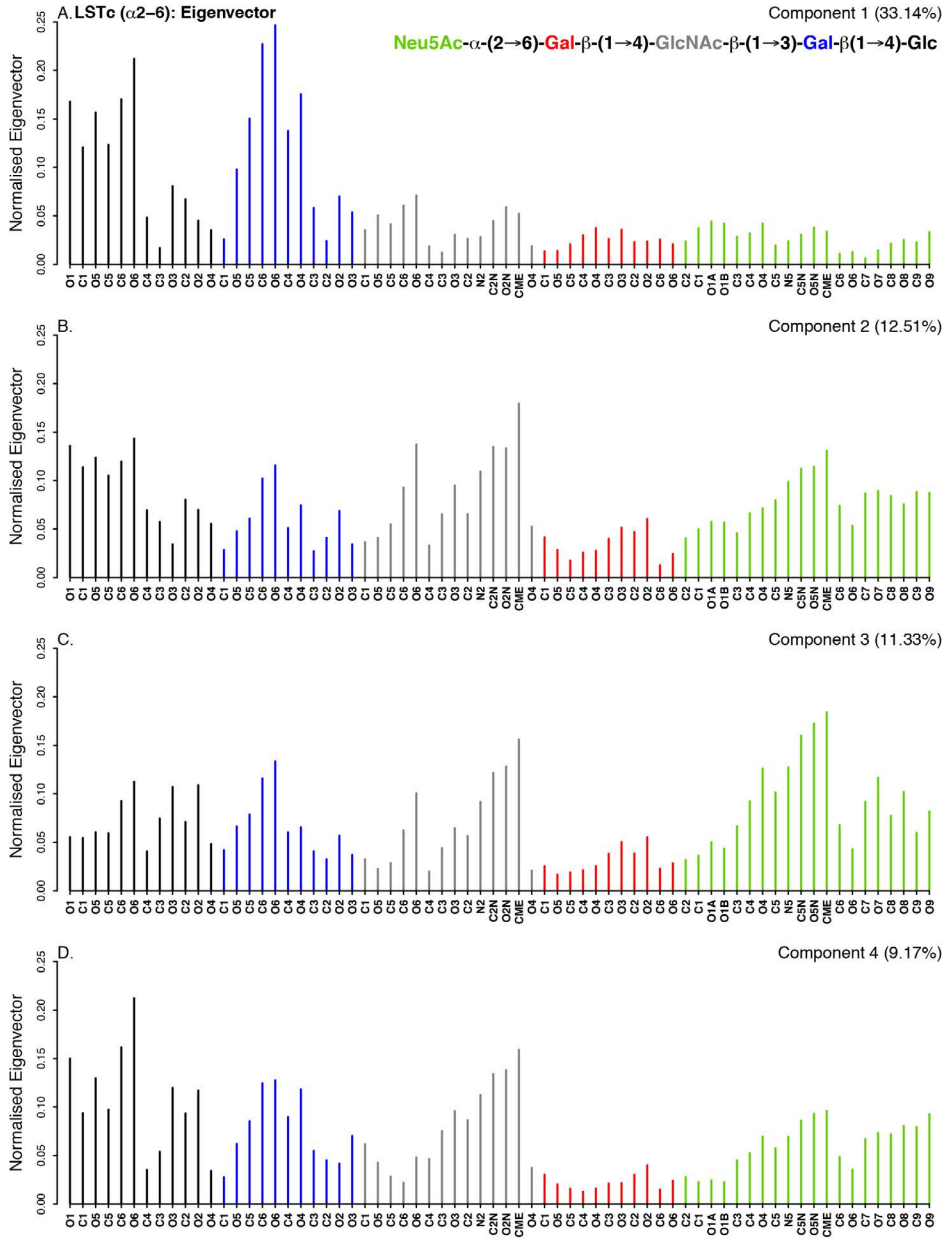

Supplementary Figure 28. *PCA normalised eigenvector plot for the analysis of the LSTc MD simulation. The colours indictate the parent monosaccharide of the atom as represented in the glycan name at the top of the figure.*

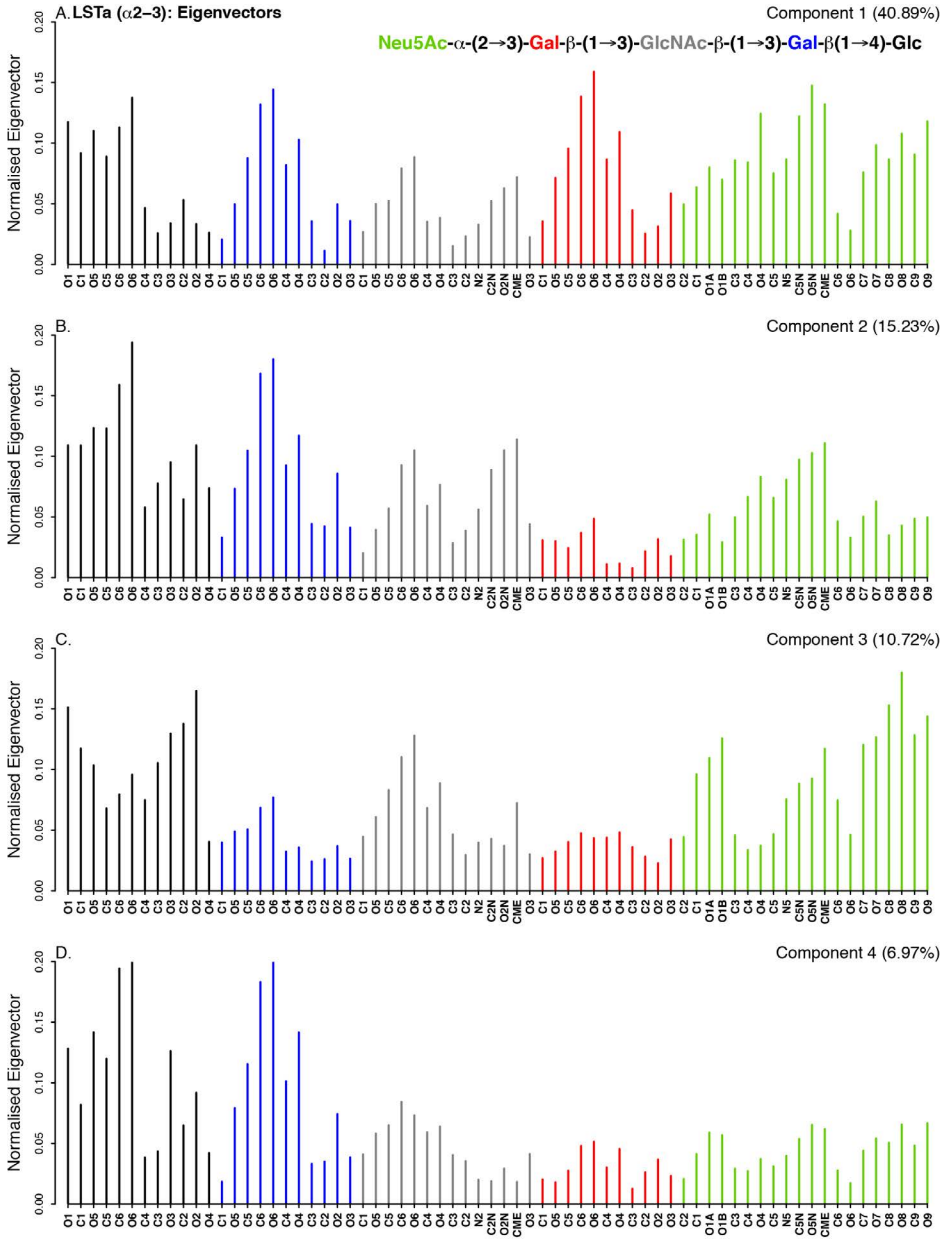

Supplementary Figure 29. *PCA normalised eigenvector plot for the analysis of the LSTa MD simulation. The colours indictate the parent monosaccharide of the atom as represented in the glycan name at the top of the figure.*

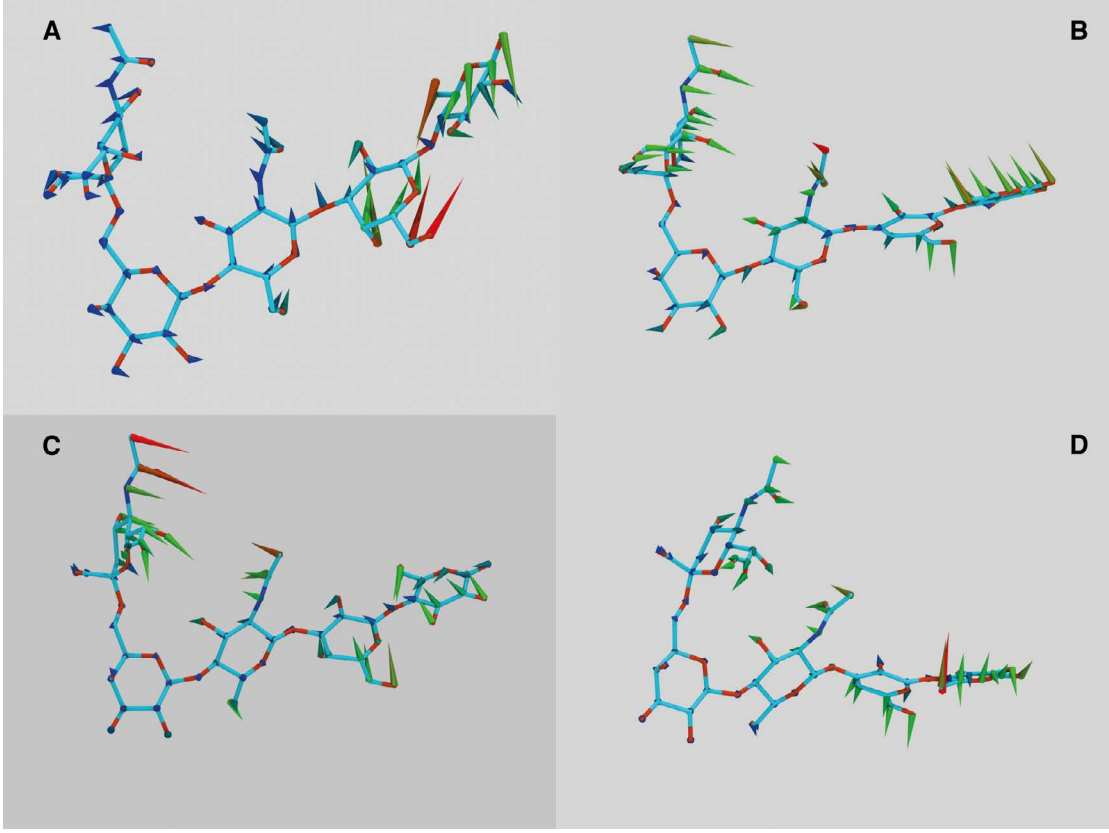

Supplementary Figure 30. *Porcupine plot representations of the first four eigenvectors for LSTc.* The first four distinct modes of motion revealed by PCA are illustrated in panels A-D (Components 1 - 4).The direction, size and colour of the spines are proportional to the direction and the magnitude of the atom motion.

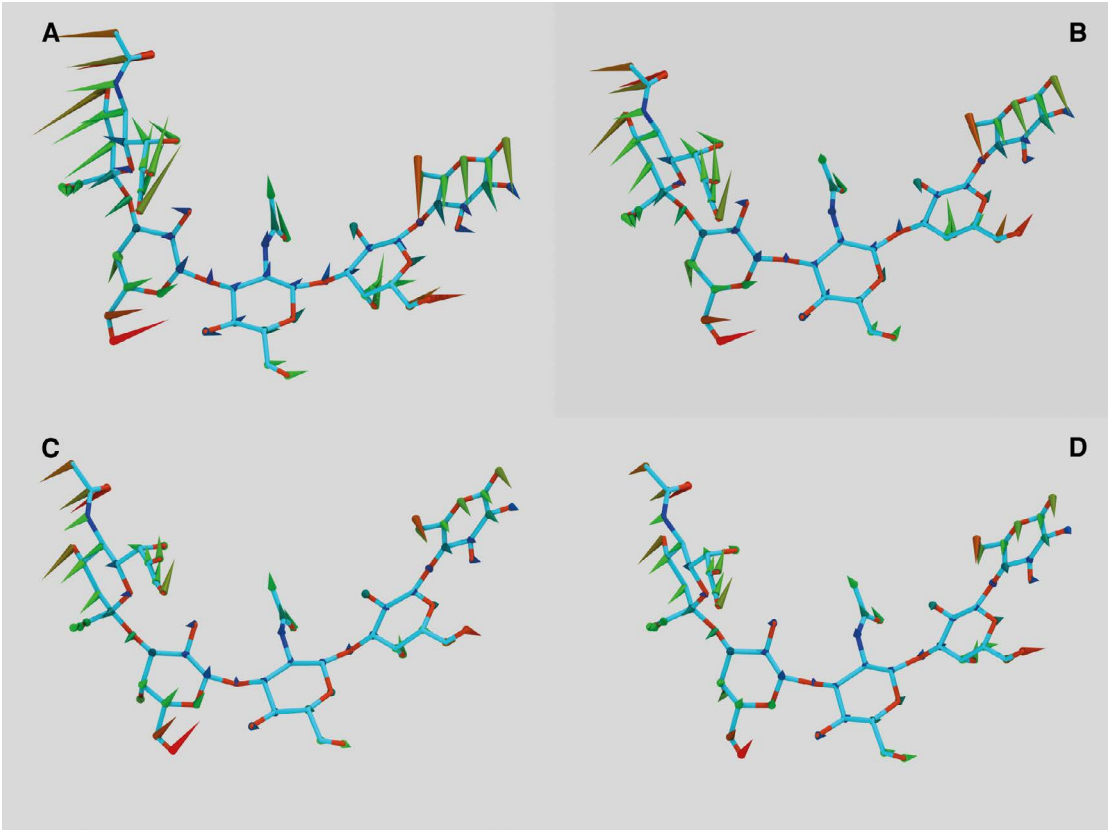

Supplementary Figure 31. *Porcupine plot representations of the first four eigenvectors for LSTa.* The first four distinct modes of motion revealed by PCA are illustrated in panels A-D (Components 1 - 4).The direction, size and colour of the spines are proportional to the direction and the magnitude of the atom motion.

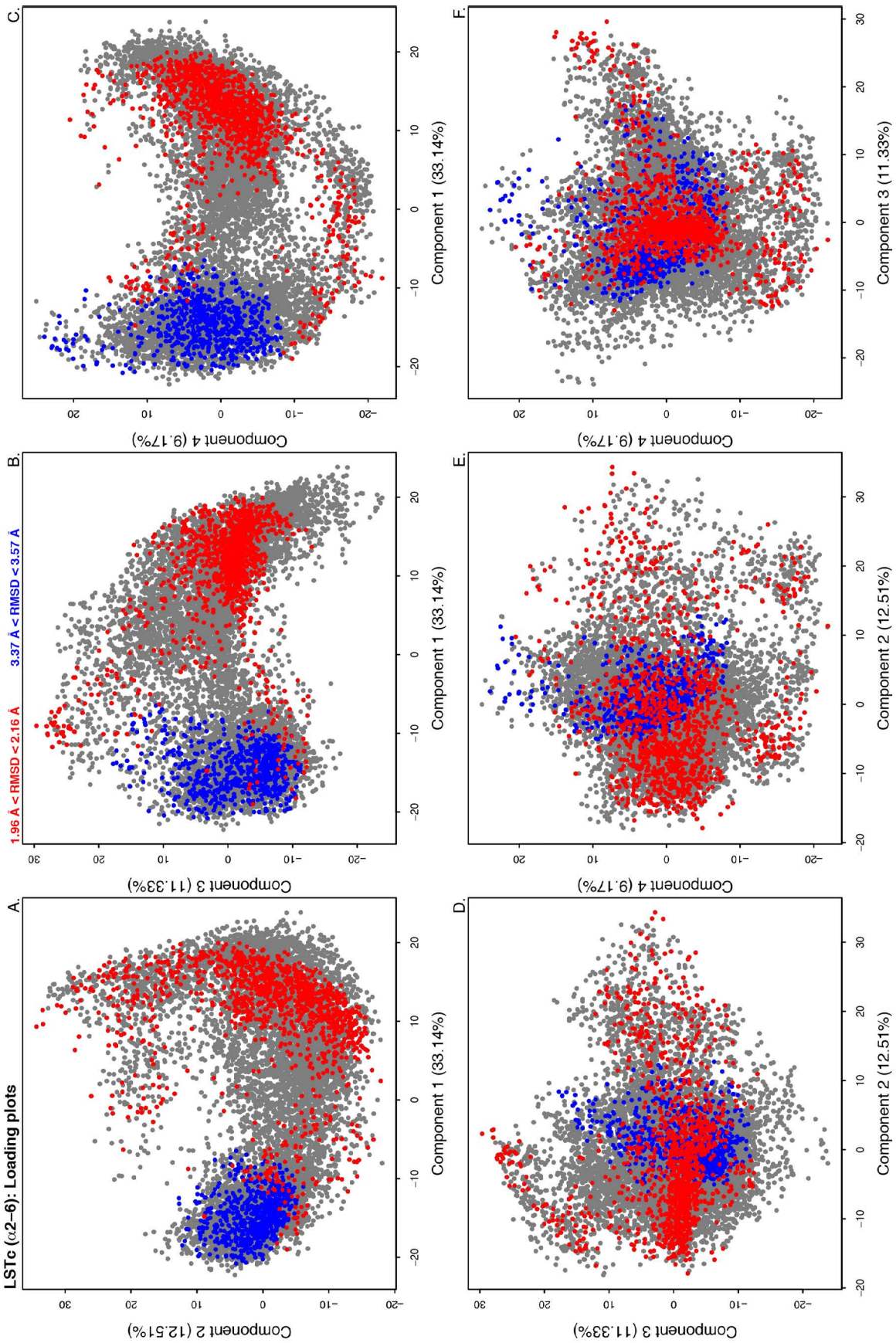

Supplementary Figure 32. *PCA Loading plot for the analysis of the LSTc MD simulation.* The red dots correspond to the conformers with RMSD values between 3.37 Å < RMSD < 3.57 Å, while the blue dots correspond conformers with RMSD values between 1.96 Å < RMSD < 2.16 Å.

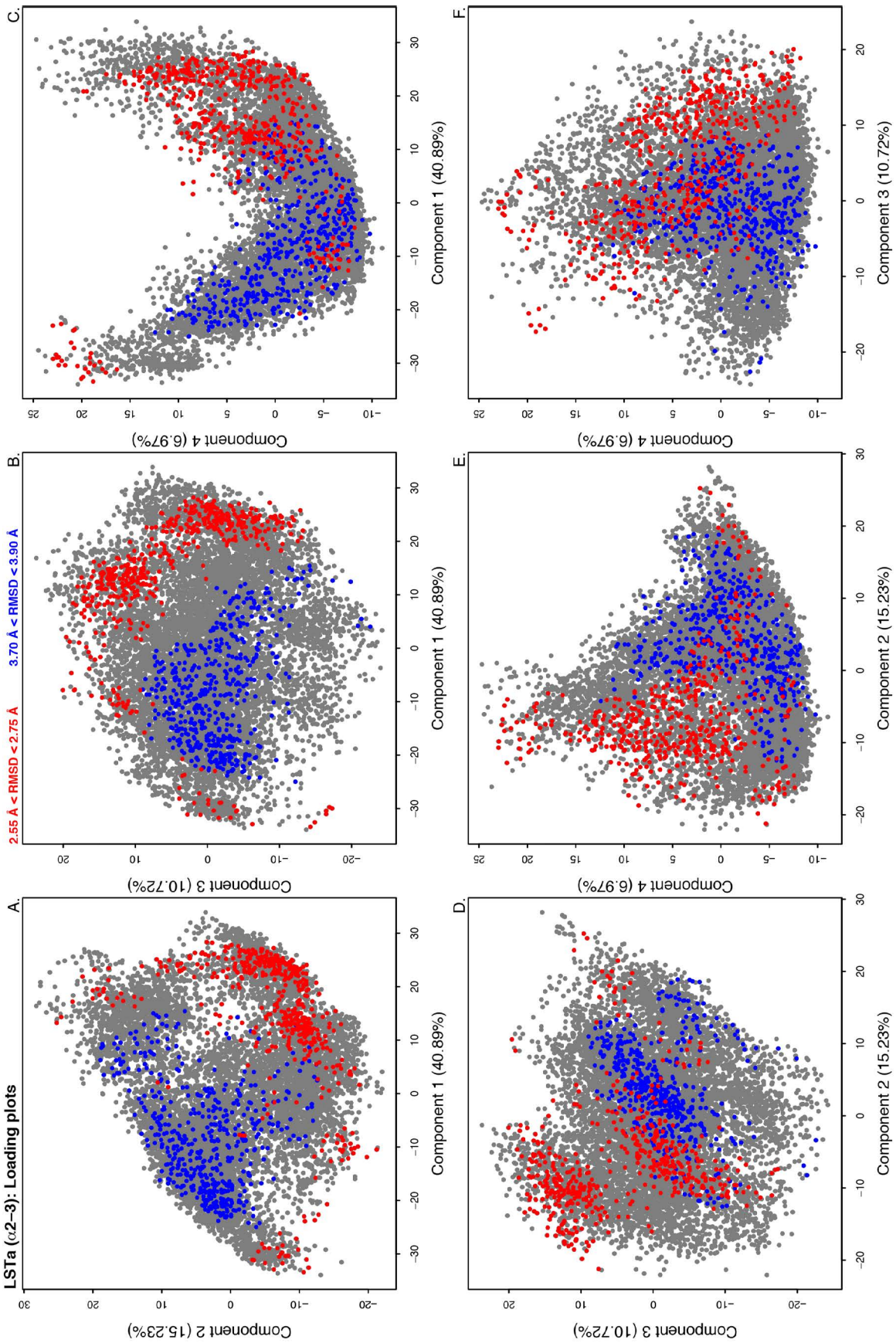

Supplementary Figure 33. *PCA Loading plot for the analysis of the LSTa MD simulation*. The red dots correspond to the conformers with RMSD values between 2.55 Å < RMSD < 2.75 Å, while the blue dots correspond conformers with RMSD values between 3.70 Å < RMSD < 3.90 Å.

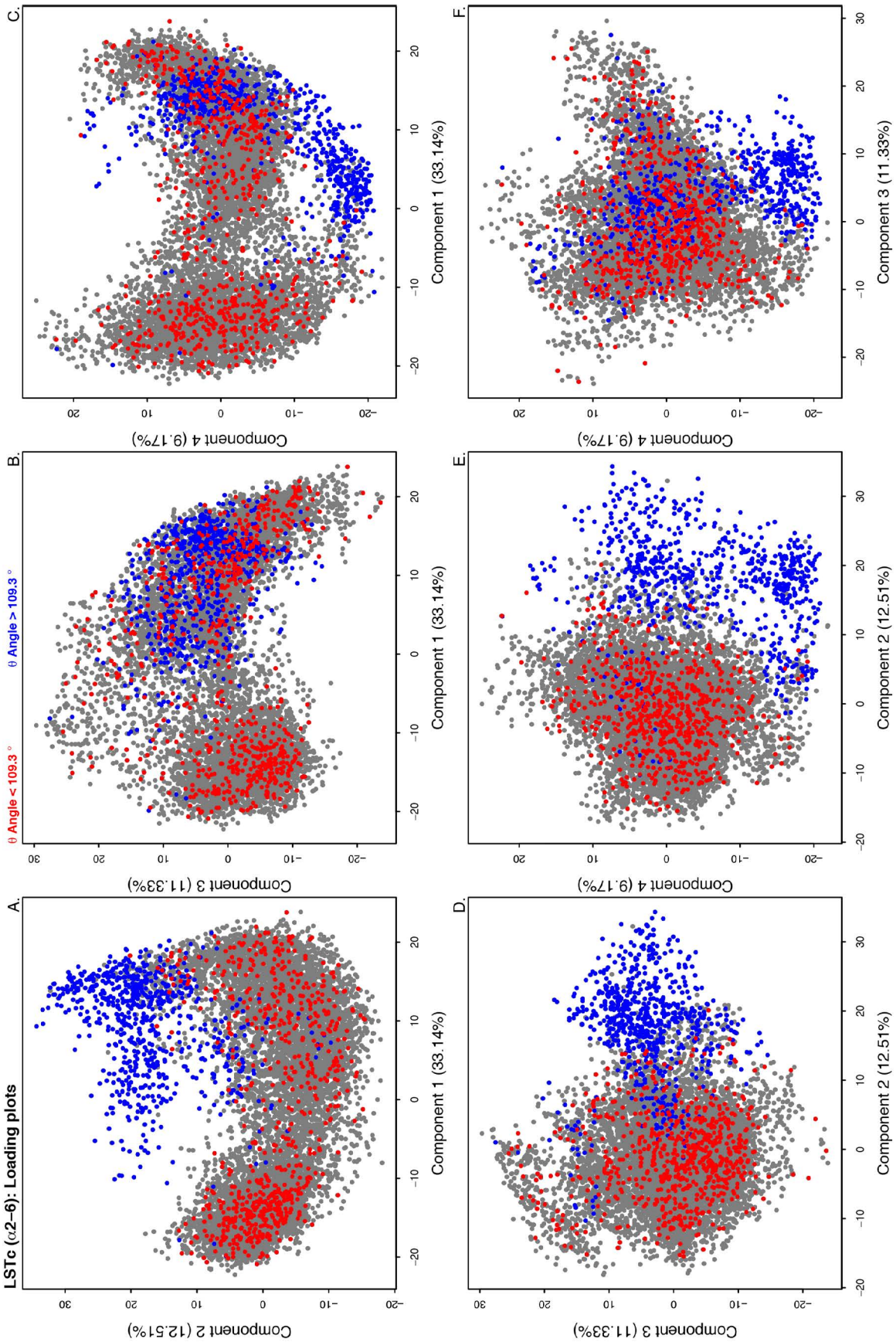

Supplementary Figure 34. *PCA Loading plot for the analysis of the LSTc MD simulation*. The red dots correspond to a subset of conformers with a θ angle < 109.3°, while the blue dots correspond to a subset of conformers with a θ angle >109.3°.

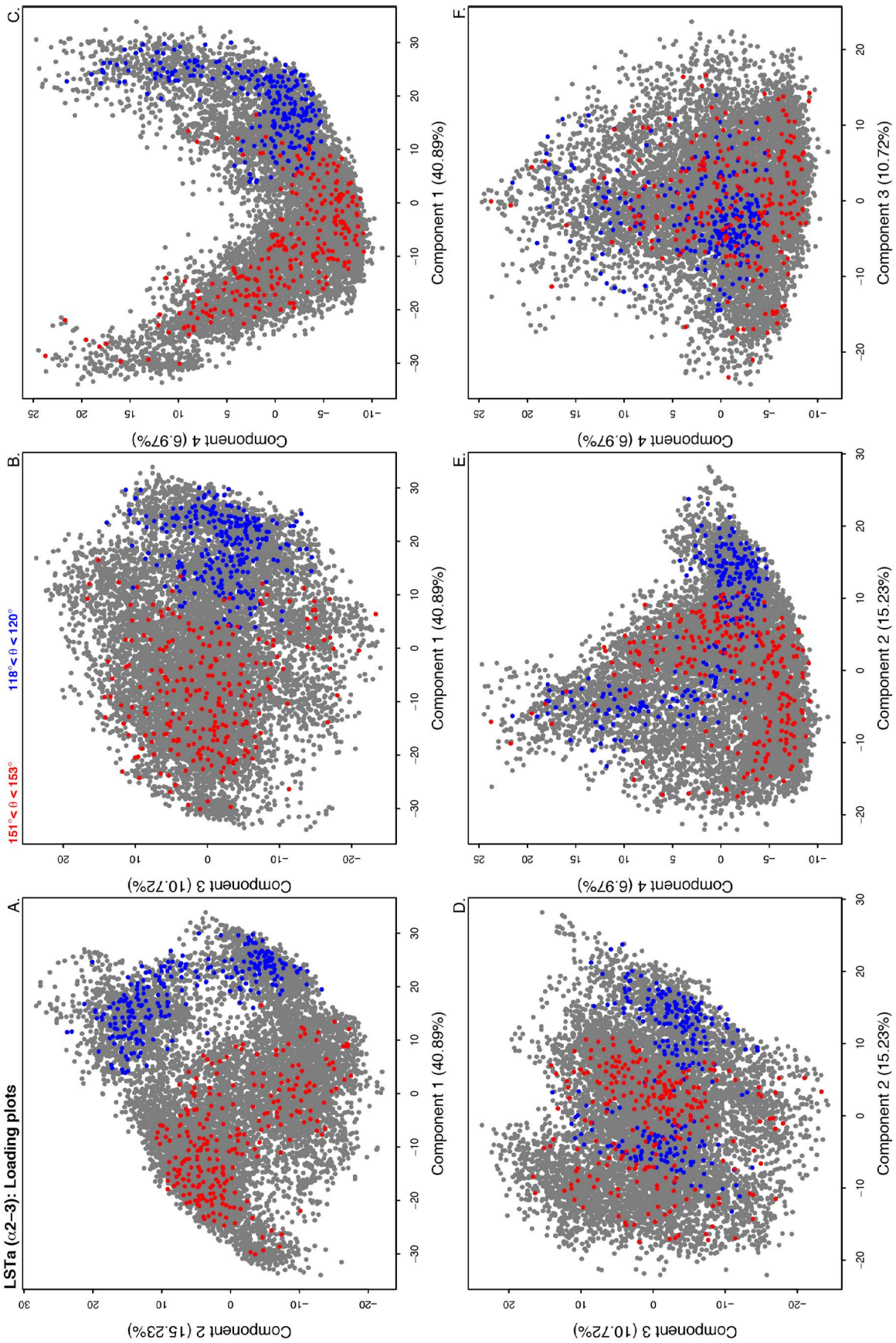

Supplementary Figure 35. *PCA Loading plot for the analysis of the LSTa MD simulation.* The red dots correspond to a subset of conformers in the range 152° < θ angle < 153° , while the blue dots correspond to a subset of conformers with the range 118° < θ angle < 120°.

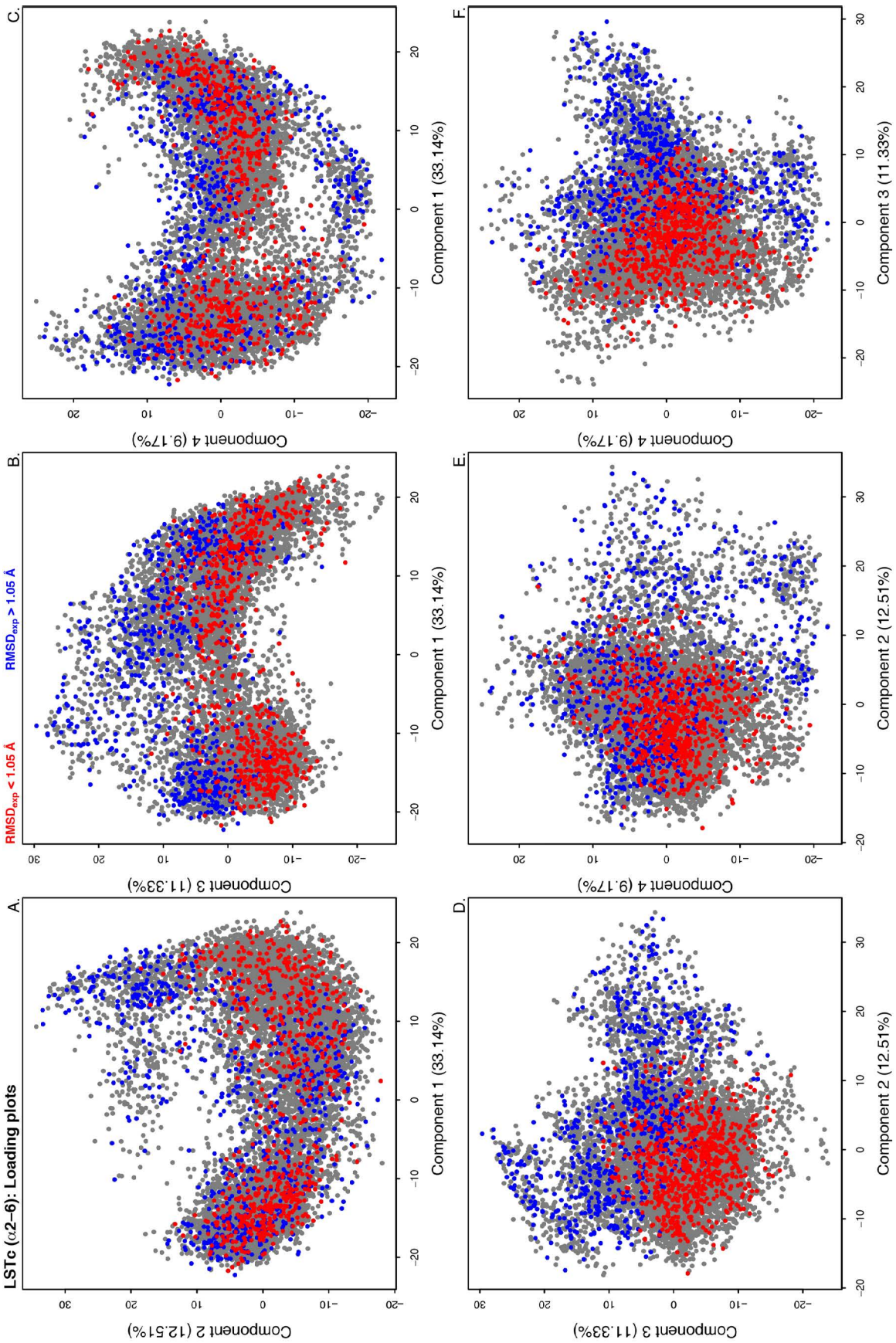

Supplementary Figure 36. *PCA Loading plot for the analysis of the LSTc MD simulation*. The red dots correspond to a subset of conformers with a $RMSD_{exp} < 1.05$ Å, while the blue dots correspond to a subset of conformers with a $RMSD_{exp} > 1.05$ Å.

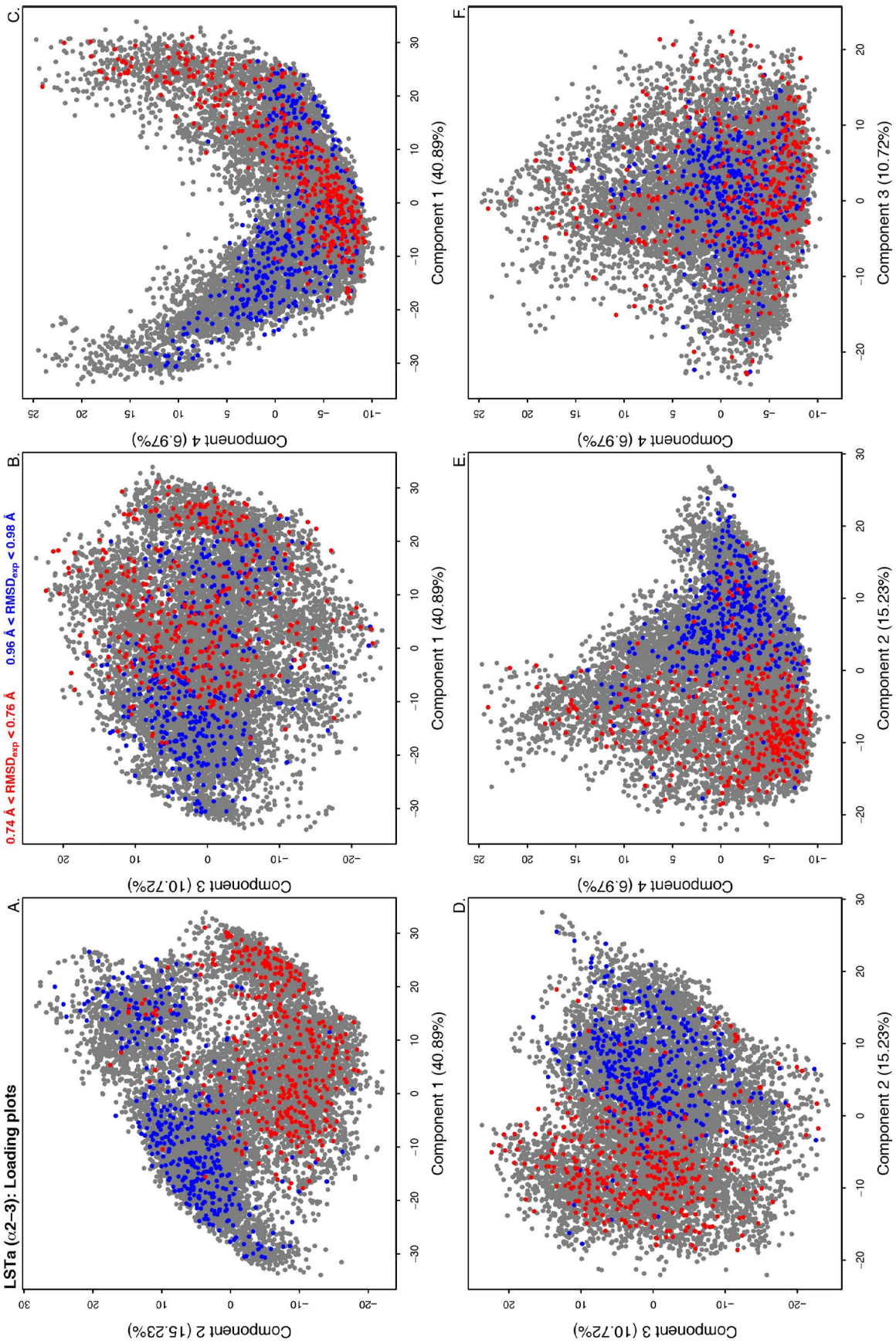

Supplementary Figure 37. *PCA Loading plot for the analysis of the LSTa MD simulation*. The red dots correspond to a subset of conformers in the range 0.74 Å < RMSDexp < 0.76 Å, while the blue dots correspond to a subset of conformers in the range 0.96 Å < RMSDexp < 0.98 Å.

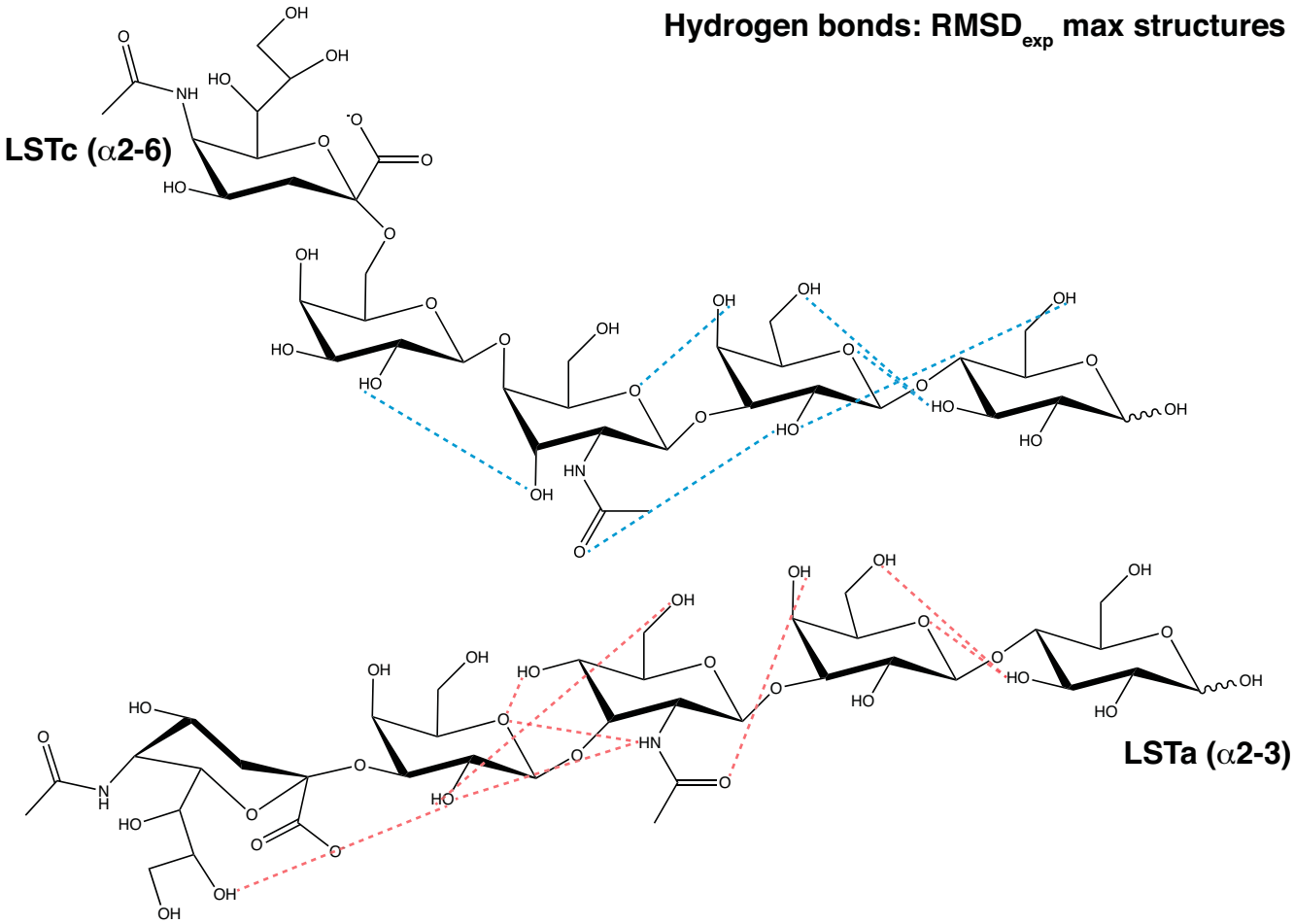

Supplementary Figure 38. *Proposed hydrogen bond network for LSTc and LSTa RMSD$_{exp}$ max conformers*. The hydrogen bond network at the non-reducing end of each glycan is strongly affected by the different linkage between Neu5Ac and Gal1; LSTa, α(2→3) and LSTc, α(2→6). The acceptor and donor atoms lie within 2.6 Å of each other and the angle between X-H••••Y (X-donor and Y-acceptor) was greater than 110˚ tending towards 180˚.